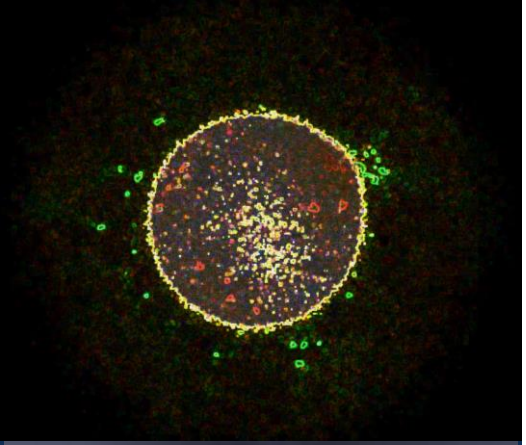

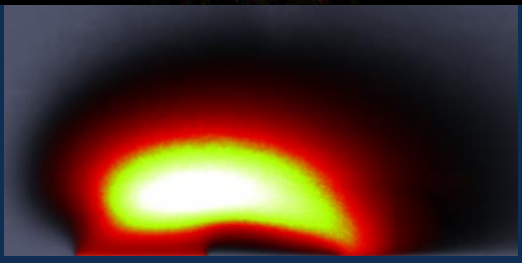

Introduction to Collisional PIC Methods for Simulating Vacuum Arcs

Matthew M. Hopkins (Sandia National Laboratories)

5th International Workshop on Mechanisms of Vacuum Arcs (MeVArc), September 1, 2015, Helsinki, Finland

Sandia National Laboratories

Exceptional service in the national interest

U.S. DEPARTMENT OF ENERGY

NNSA National Nuclear Security Administration

Sandia National Laboratories is a multi-program laboratory managed and operated by Sandia Corporation, a wholly owned subsidiary of Lockheed Martin Corporation, for the U.S. Department of Energy's National Nuclear Security Administration under contract DE-AC04-94AL85000. SAND NO. 2011-XXXXP

Vacuum Arcs?

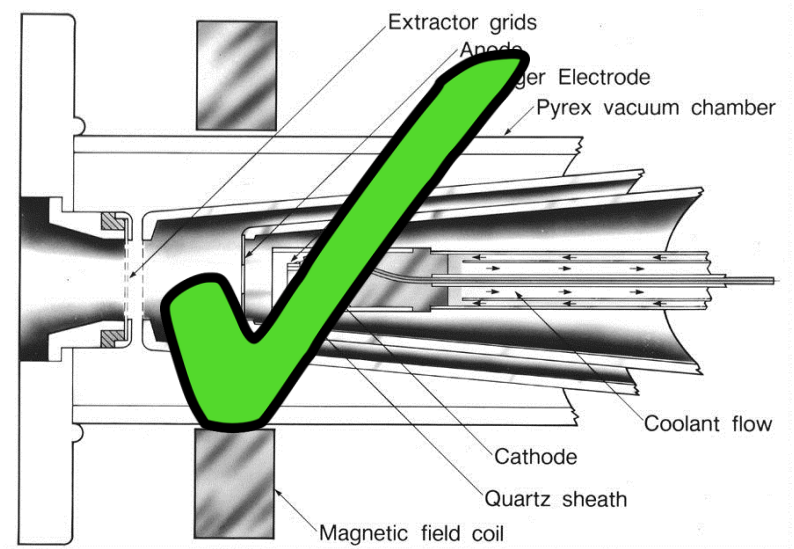

Simplified schematic of the LBNL Mevva II ion source, from Ian Brown, "Vacuum arc ion sources: A review", XXVth ISDEIV, Tomsk, Russia, 2012.

CLIC accelerating cavities.

Also: sp ons, high voltage br in vacuum electro

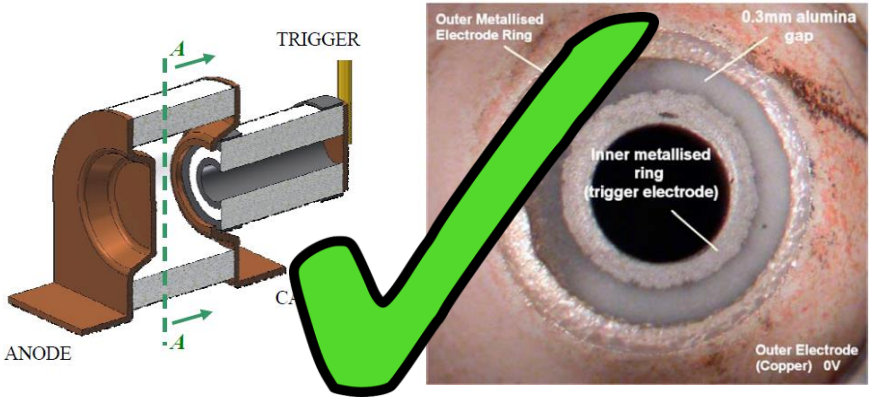

Sprytrons. Taken from B M Coaker, C Bell, R J Seddon, and J S Bower, "Miniature triggered vacuum switches for precise initiation of insensitive loads in demanding environments", 39th ICOPS, Edinburgh, UK, 2012.

Outline

I. Cartoon of Vacuum Arc Process
II. Boltzmann Equation
III. Particle-in-Cell (PIC)
IV. Direct Simulation Monte Carlo (DSMC)
V. Examples: 1D
VI. Electrode Models
VII. Examples: 2D, 3D
VIII. Recent Advance

Cartoon of Vacuum Arc Discharge Evolution

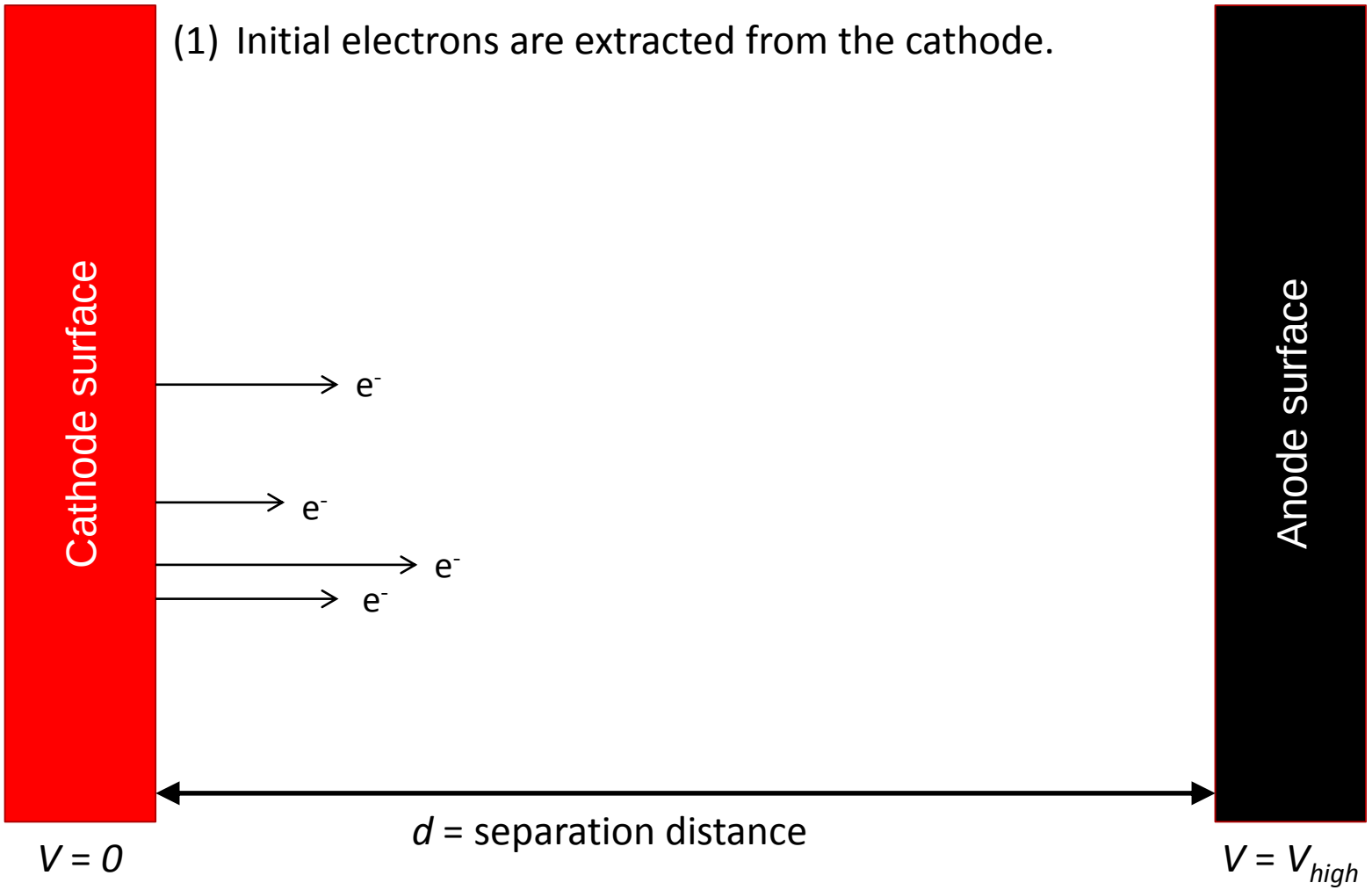

Cartoon of Vacuum Arc Discharge Evolution

(1) Initial electrons are extracted from the cathode.
(2) Electrons accelerate and some find a neutral to ionize.
(There is no perfect vacuum. Cathodes are imperfect.)

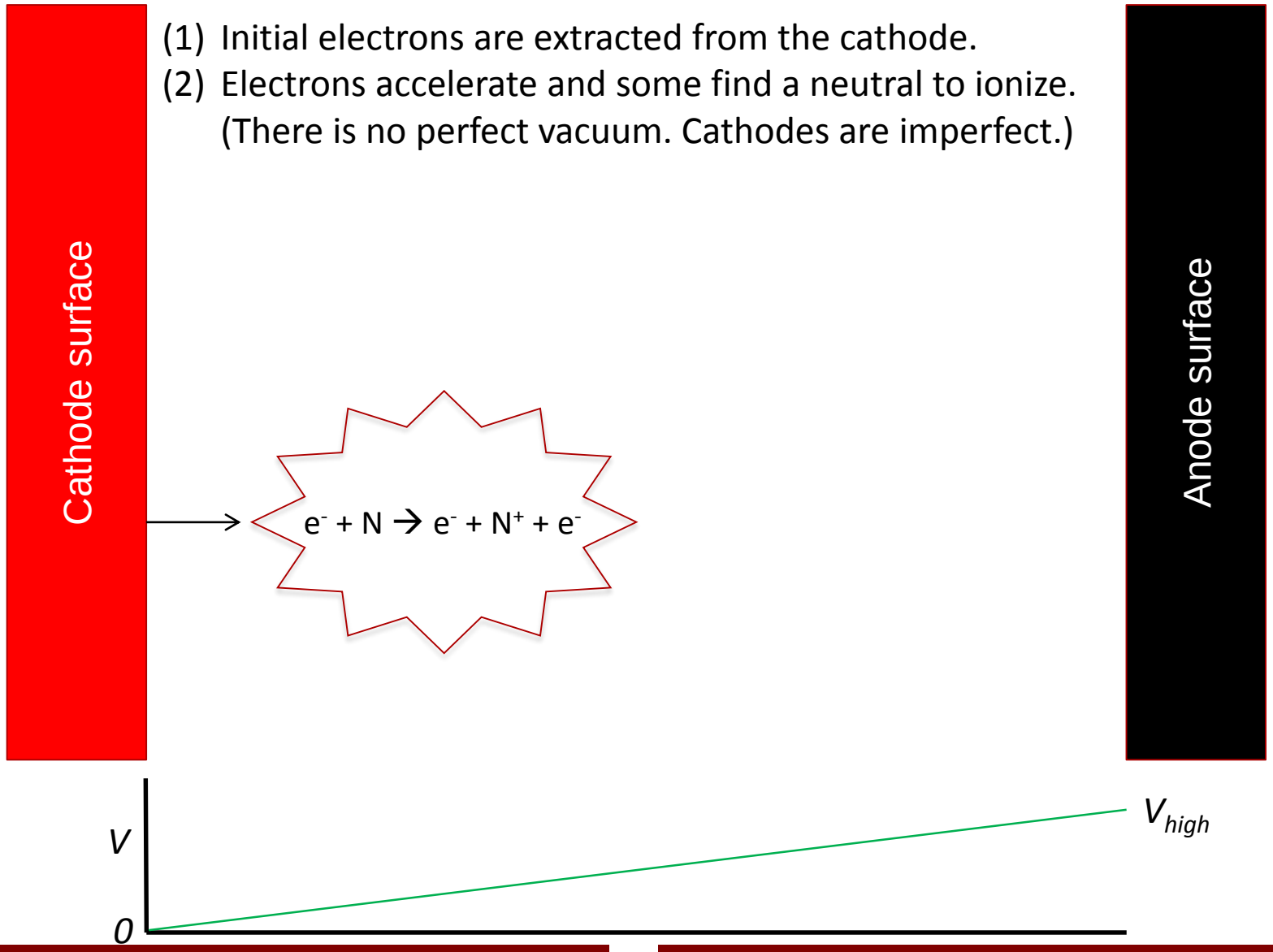

Cartoon of Vacuum Arc Discharge Evolution

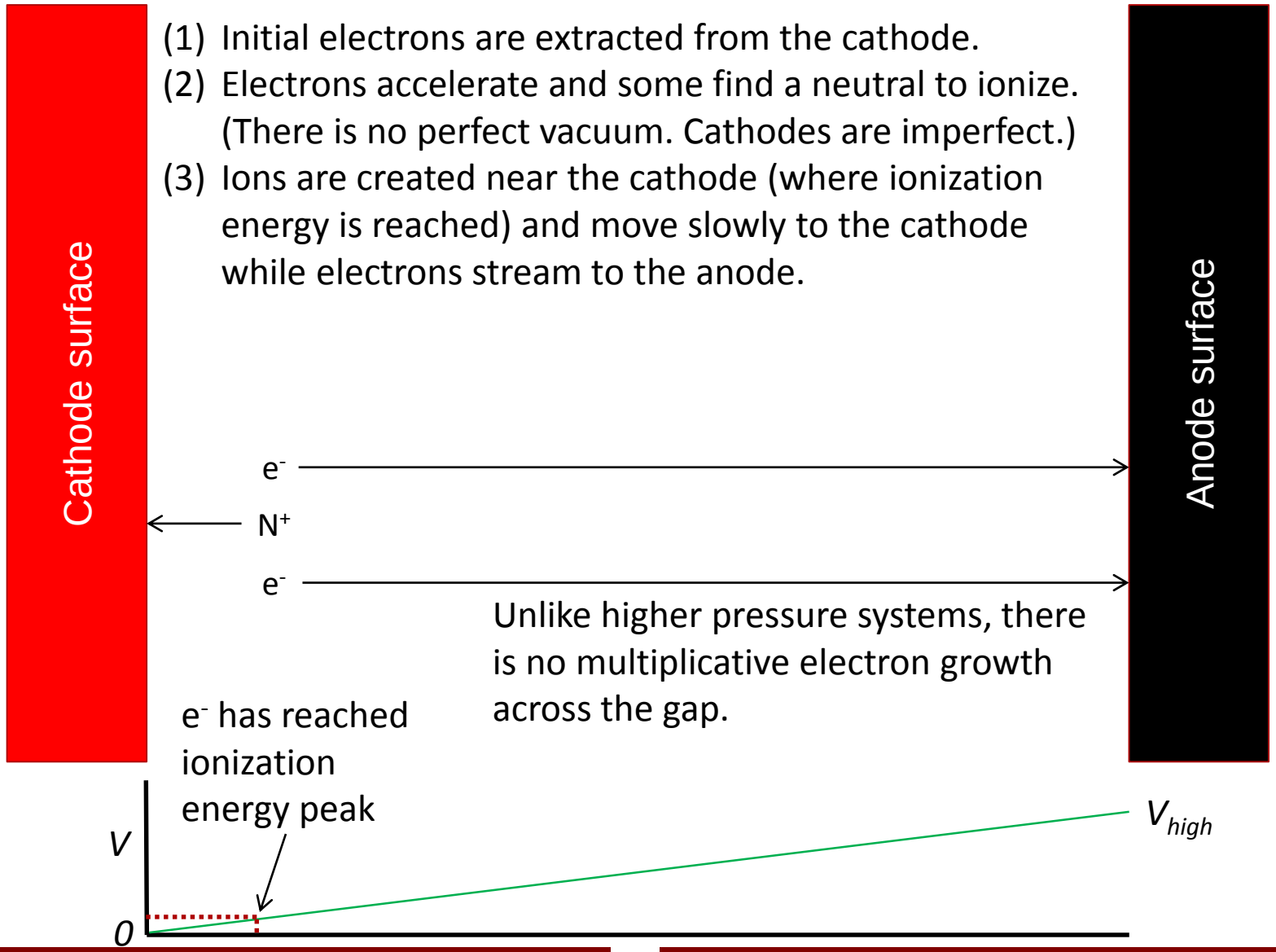

Cartoon of Vacuum Arc Discharge Evolution

(3) Ions are created near the cathode (where ionization energy is reached) and move slowly to the cathode.

(4) A cathode plasma begins to grow due to accumulation of ions near cathode surface.

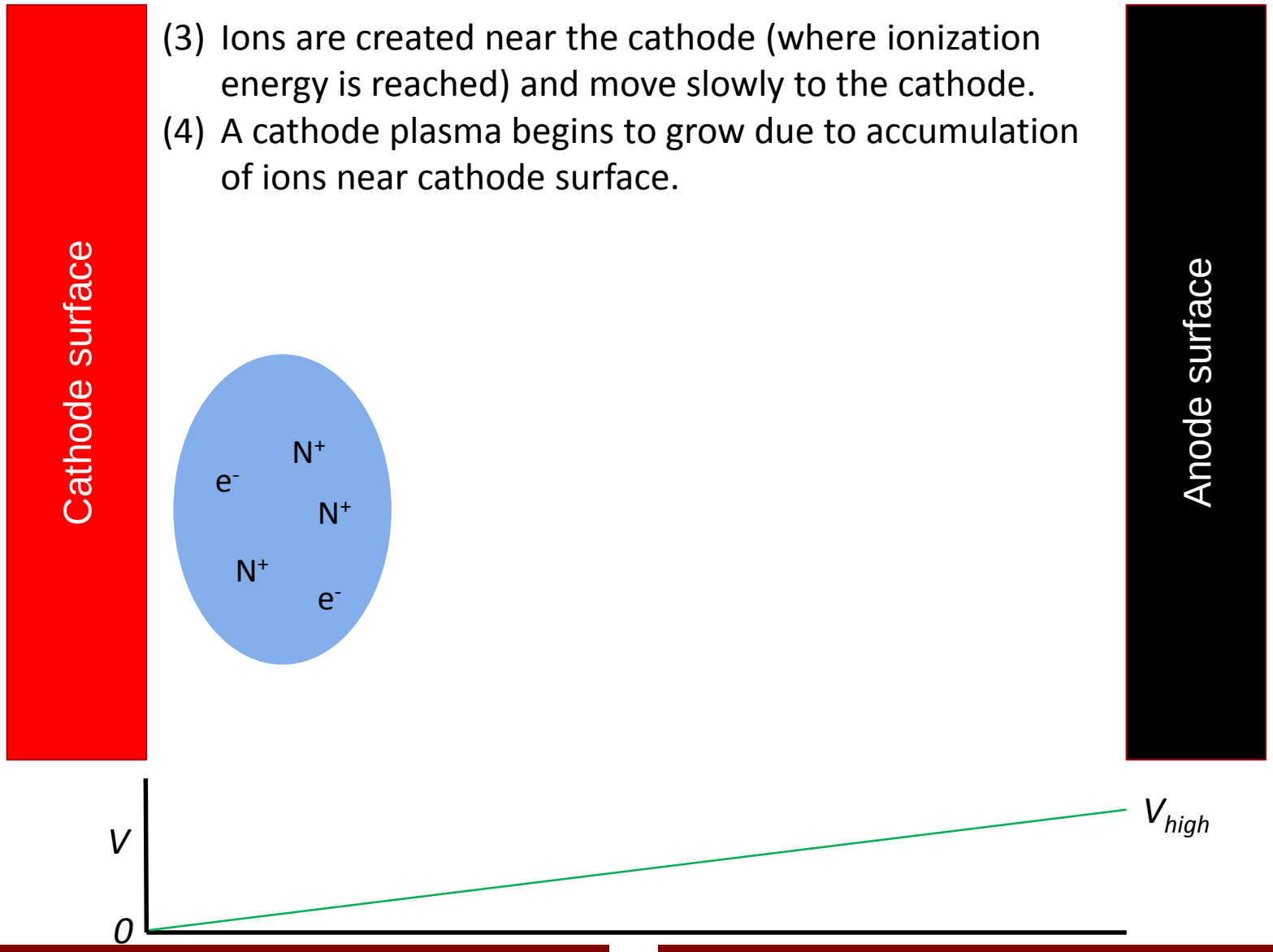

Cartoon of Vacuum Arc Discharge Evolution

Sandia National Laboratories

Cathode surface

(4) A cathode plasma begins to grow due to accumulation of ions near cathode surface.

(5) Additional growth occurs due to secondary electron and neutral emission from ion impact on cathode. A multiplicative surface-based process takes place growing the cathode plasma.

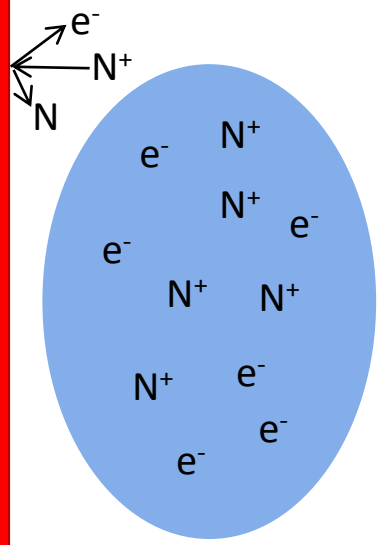

Growth factors:

- Ion impact leads to increased neutral and electron emission.
- Surface heating leads to increased neutral and electron emission.
- Increased neutral density leads to increase in ions due to ionization.

Anode surface

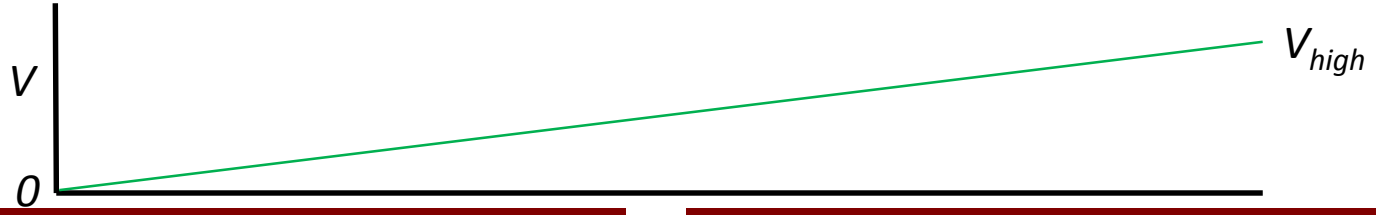

Cartoon of Vacuum Arc Discharge Evolution

(5) Additional growth occurs due to secondary electron and neutral emission from ion impact on cathode. A multiplicative surface-based process takes place growing the cathode plasma.

(6) Plasma density increases to the point it modifies the local field. Still growing via positive feedback.

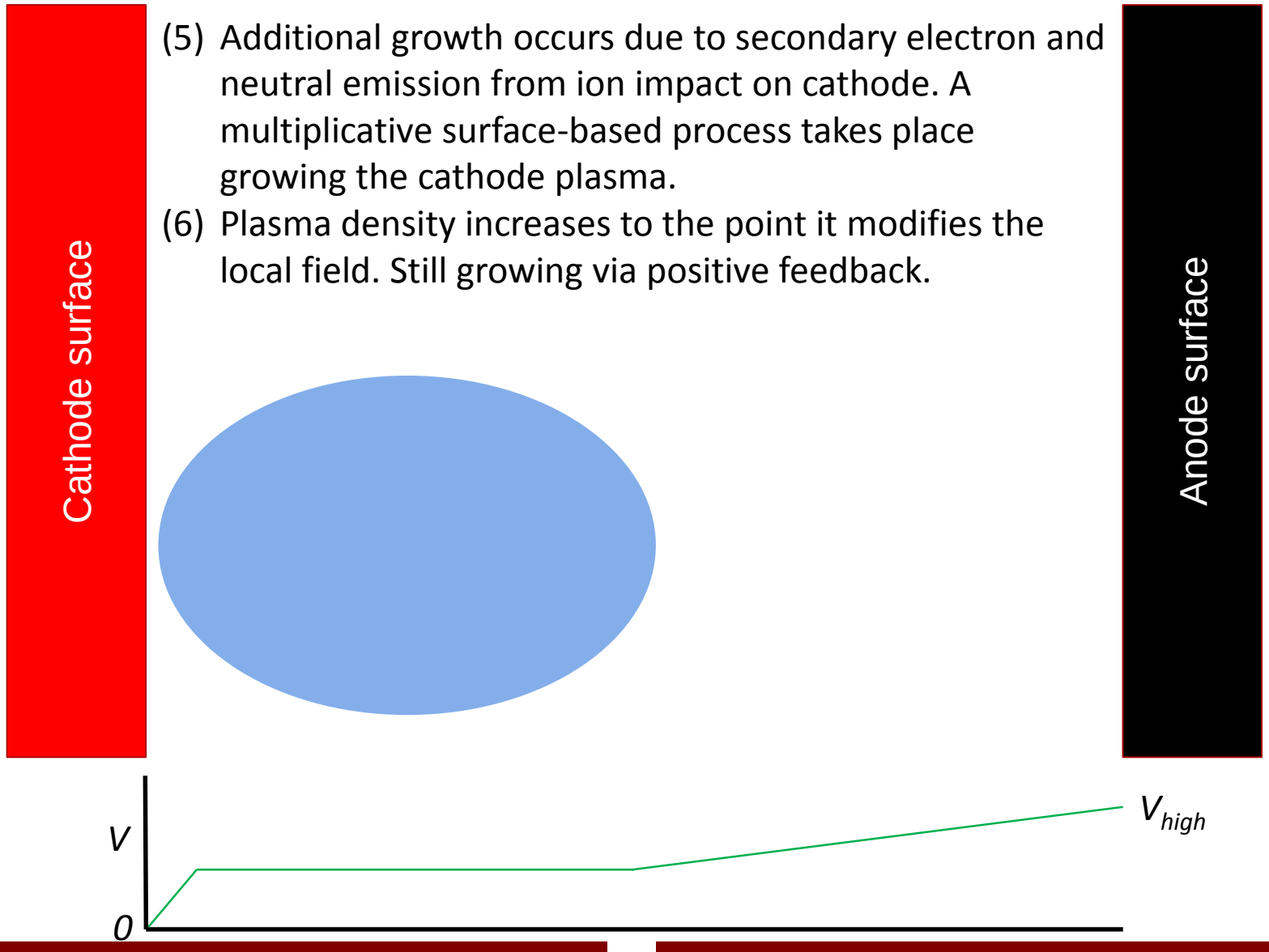

Cartoon of Vacuum Arc Discharge Evolution

(6) Plasma density increases to the point it modifies the local field.

(7) Explosive growth occurs as the field in the cathode sheath achieves Fowler-Nordheim (cold field emission) threshold. Plasma size and density grows to form conducting path → arc.

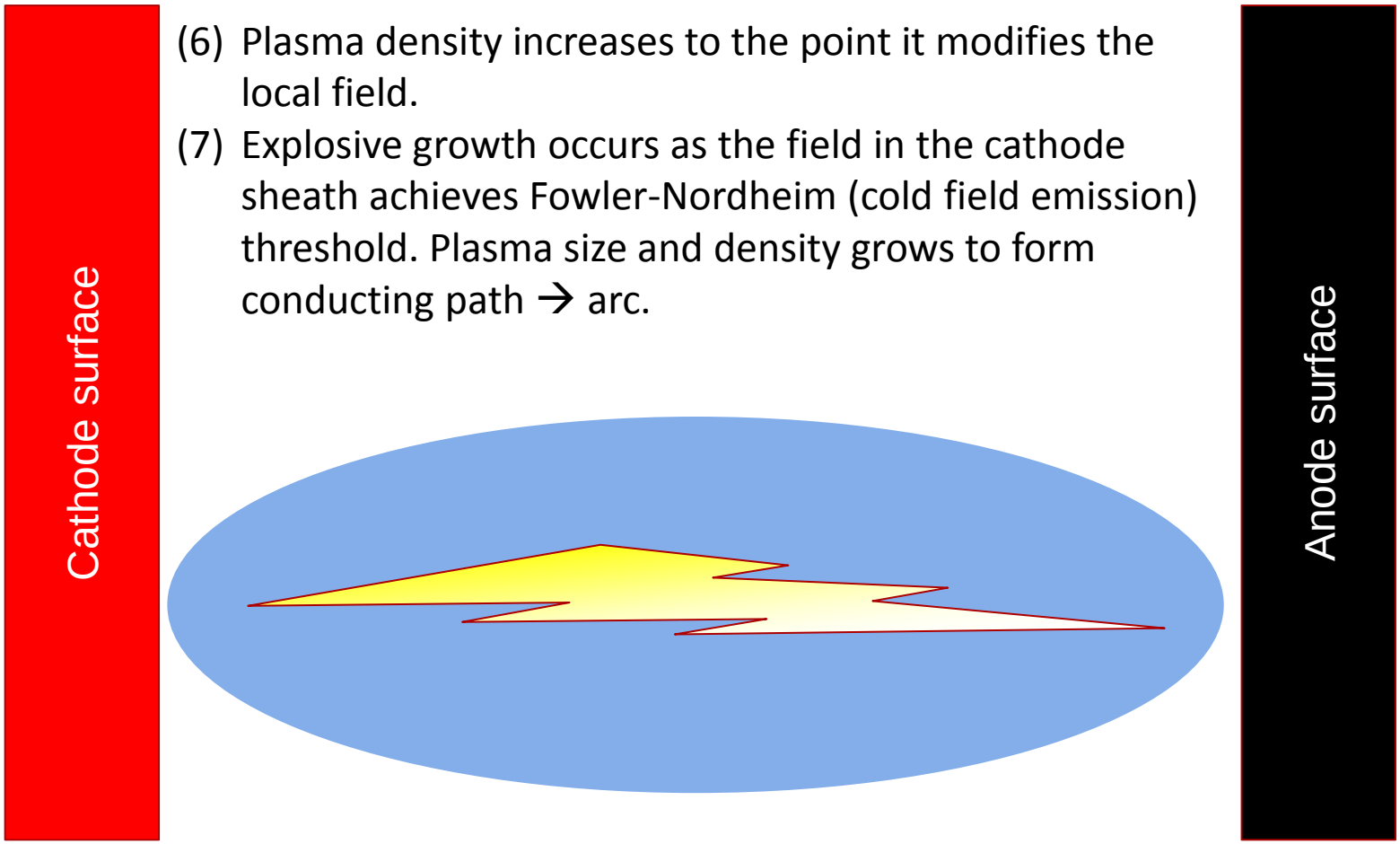

Physics Modeling Requirements

- Electrostatics.
- Kinetic description, especially for electrons.
- Electron chemistry (elastic collisions, ionization, excitation, photoemission).
- Neutral-ion elastic collisions.
- Photoemission / photoelectric current.
- Driving circuit.
- Surface response to fields, temperature, ion impact.

At SNL, we use some combination of:

- Direct Simulation Monte Carlo (DSMC): collision framework.
- Particle-in-Cell (PIC): couples charged particles and fields.
- Finite element method for electrostatics. Other treatments recommended if you can do so (e.g., finite difference method on a Cartesian mesh).

The Boltzmann Equation

The particle methods we use generate solutions to the Boltzmann equation,

$$\frac{\partial f}{\partial t} + v \cdot \nabla_x f + F \cdot \nabla_v f = \left(\frac{\partial f}{\partial t} \right)_{coll}$$

where

$f(x, v, t)$ = distribution function in phase space,
x = particle location,
v = particle velocity,
F = external applied force, and
$(\partial f / \partial t)_{coll}$ represents changes due to particle collisions.

For example, $n(x,t) = \int f(x,v,t) dv$.

In 3D the Boltzmann equation is 7-dimensional (!).

The Boltzmann Equation

Repeating: in 3D the Boltzmann equation is 7-dimensional (!).

We discretize the Boltzmann equation in space and time. We discretize the spatial portion of *(x, v)* phase space by employing a mesh. We discretize in time by using a time integration method over discrete time steps t_n, t_{n+1}, … This effectively reduces the problem to evolving the velocity distribution function in each cell and over each time step:

$$f\left(x_{cell}, t_n, v\right) \rightarrow f\left(x_{cell}, t_{n+1}, v\right), \text{ or}$$

$$f_{cell,n}(v) \rightarrow f_{cell,n+1}(v)$$

where the second line demonstrates how we generally use "*f*" to mean the velocity distribution function (vdf). We also often use *f* as if it were an energy distribution function. And we often drop the explicit connection to the discretization.

The Boltzmann Equation

We approximate *f(v)* in each cell by a discrete set of particles with individual velocities. Because the physical number of particles in a cell can be quite large, we will further approximate the vdf by assuming each computational particle (or notional particle) represents some number of real ones. This ratio is referred to as the "macroparticle weight" or just "particle weight", w_p.

The basic solution methodology advances a set of computational particles in a mesh from one discrete time to another accounting for particle motion, particle forces, and particle collisions. Unlike continuum methods where densities, velocities, energies, etc., are the primary "solution variables", the primary "solution variables" in the kinetic methods we use are particle positions and particle velocities. *Everything else is derived from this.*

The Boltzmann Equation

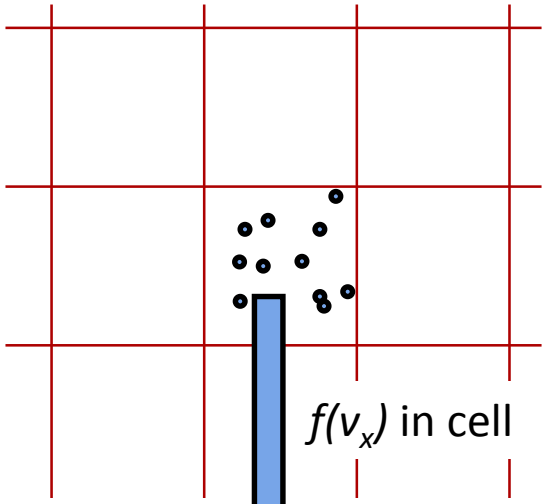

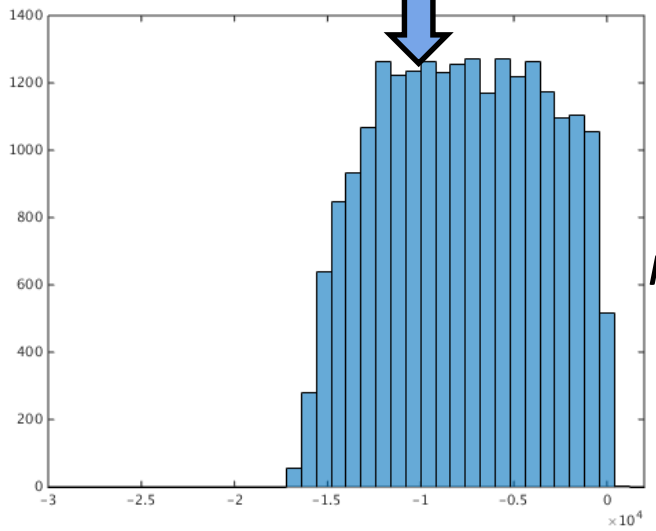

$$n = \sum_{particles} w_p f(v_x)$$

$$nv_x = \sum_{particles} w_p v_x f(v_x)$$

$$\vdots$$

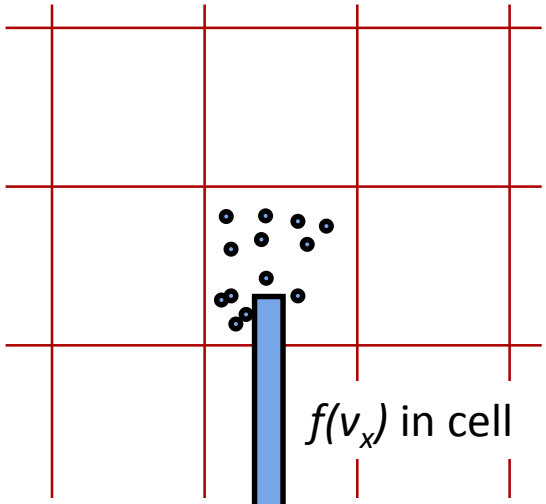

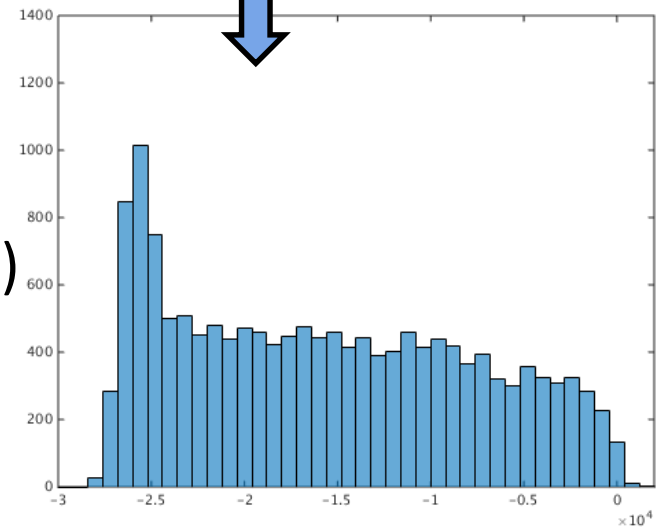

Particle-in-Cell (PIC)

PIC is focused on part of the Boltzmann equation,

$$\frac{\partial f}{\partial t} + v \cdot \nabla_x f + F \cdot \nabla_v f = \left(\frac{\partial f}{\partial t}\right)_{coll}$$

where PIC typically assumes collisionless particles (RHS = 0). Replacing *F* with electric and magnetic forces,

$$\frac{\partial f}{\partial t} + v \cdot \nabla_x f + \frac{q}{m}\left(E + v \times B\right) \cdot \nabla_v f = 0$$

gives us the Vlasov equation with *q* the particle charge, *E* the electric field, and *B* the magnetic field. We consider the electrostatic (ES) case where we assume *B* = 0,

$$\frac{\partial f}{\partial t} + v \cdot \nabla_x f + \frac{qE}{m} \cdot \nabla_v f = 0$$

and will couple to Poisson's equation, although there are many electromagnetic (EM) PIC codes that couple to Maxwell's equations and solve for a consistent *B*.

Particle-in-Cell (PIC)

In addition to integrating charged particle trajectories, we need to solve Poisson's equation,

$$\nabla\left(\varepsilon_0 \nabla V\right) = -\rho = q_e\left(n_{i,total} - n_e\right)$$

where ε_0 is the permittivity of free space, $n_{i,total}$ is total ion number density (assuming only single ionizations) and n_e is electron number density. We generally don't care about V directly but need to compute the electric field, $E = -\nabla V$.

There are many ways to solve Poisson's equation. If using a Cartesian mesh with fixed spacing a finite difference method (FDM) is a great choice, e.g., in 1D,

$$\frac{V_{k-1} - 2V_k + V_{k+1}}{\Delta x^2} = \frac{q_e}{\varepsilon_0}\left(n_{i,total,k} - n_{e,k}\right)$$

where k subscripts indicate the values at grid point k and Δx is the mesh spacing. Note the lack of a time derivative.

Particle-in-Cell (PIC)

Much of the diversity of PIC methods involves evaluating the RHS of

$$\frac{V_{k-1} - 2V_k + V_{k+1}}{\Delta x^2} = \frac{q_e}{\varepsilon_0}\left(n_{i,k} - n_{e,k}\right)$$

in different ways. Methods are “nearest neighbor”, “cloud-in-cell”, etc., and they resolve to being higher order approximations to the discrete particle charge distribution. Higher order approximations require larger computational stencils.

Once *V* is available, there are a number of ways to compute *E* at the particle locations. Again, they are of different orders and require growing stencils for better approximations.

There are compatibility constraints between the charge-to-grid and field-to-particle interpolations.

Particle-in-Cell (PIC)

- Because of the elliptic Poisson equation the overall method is globally coupled and requires solution of a global linear system. This has considerable impact on parallel implementations and performance. It can also cause instantaneous “action-at-a-distance”. For finite perturbation speed you need to use an EM method.

- The methodology described here is explicit in time. There are methods that are semi-implicit, and even fully implicit.

- Particle weight w_p is used for computing charge density, but not inertial response (e.g., it’s not really a “heavy” particle).

Particle-in-Cell (PIC)

Basic ES PIC iteration to advance from time step *n* to *n+1* uses a time-splitting method:

1. Update particle velocities over $\Delta t/2$ and positions with Δt,

$$v_i^{\text{å}} = v_i^n + \frac{q_i E^n(x_i^n)}{m_i}\frac{\Delta t}{2}$$

$$x_i^{n+1} = x_i^n + v_i^{\text{å}}\Delta t$$

2. Solve Poisson's equation to get new fields,

$$\nabla\left(\varepsilon_0 \nabla V^{n+1}\right) = -\rho = q_e(n_i^{n+1} - n_e^{n+1})$$

$$E^{n+1} = -\nabla V^{n+1}$$

3. Compute final update to velocities with new forces,

$$v_i^{n+1} = v_i^{\text{å}} + \frac{q_e E^{n+1}(x_i^{n+1})}{m_i}\frac{\Delta t}{2}$$

Particle-in-Cell (PIC)

Requirements/assumptions for employing ES PIC include:

1. Cell sizes must resolve Debye length λ_D to avoid numerical heating,

$$\Delta x < \lambda_D = \sqrt{\frac{k_B T_e \varepsilon_0}{n_e q_e^2}}$$

   where k_B is the Boltzmann constant and T_e is the electron temperature.

2. Time step must resolve plasma frequency ω_p,

$$\Delta t < \frac{2}{\omega_p} = 2\sqrt{\frac{\varepsilon_0 m_e}{n_e q_e^2}}$$

3. Should satisfy Courant-Friedrichs-Lewy (CFL) condition similar to continuum CFD,

$$\Delta t < \frac{\Delta x}{v}$$

Particle-in-Cell (PIC)

Requirements/assumptions for employing ES PIC include: (cont.)

4. Electrostatic solvers usually expect some resolution of grad(V) or grad(V)^2. It is often unclear how to interpret this as there are combinations of quasi-neutral plasma, non-neutral regions, and high applied fields.

These constraints would ideally apply to the most extreme constraints (minimum λ_D, maximum ω_p, maximum v on minimum Δx), but because particle properties are stochastic this cannot be guaranteed. This is a recurring theme in kinetic particle methods.

Direct Simulation Monte Carlo (DSMC)

DSMC is focused on computing solutions to a different part of the Boltzmann equation,

$$\frac{\partial f}{\partial t} + v \cdot \nabla_x f + F \cdot \nabla_v f = \left(\frac{\partial f}{\partial t} \right)_{coll}$$

where DSMC typically assumes $F = 0$ (no external forces).

- DSMC is a completely local method. Only information within a computational cell is required. (Not true for electrostatic PIC.)
- Within a single cell actual particle locations are assumed irrelevant. All particles in the cell are candidates to collide with all other particles in a cell.
- Assume instantaneous binary collisions separate from motion.

Direct Simulation Monte Carlo (DSMC)

Sandia National Laboratories

Letting N = number of computational particles in a cell ($N = nV_c/w_p$ or $n = w_pN/V_c$), there are $N(N - 1)/2$ potential collision pairs. We could step through all of them every time step. The No Time Counter (NTC) DSMC method is a way to effectively sample the same collision pairs without doing as much work…

The probability of a computational particle moving at velocity v colliding with a randomly placed stationary computational particle in a cell of volume V_c over a time period of Δt is

$$P = \frac{v\sigma\Delta t}{V_c}$$

where here σ is assumed to be a constant cross-section. The numerator is the cylindrical volume spanned by the particle's collision cross-section over the time interval.

Direct Simulation Monte Carlo (DSMC)

Since both particles are moving, the probability of them interacting becomes

$$P_{i,j} = \frac{|v_{i,j}|\sigma\Delta t}{V_c}$$

where $v_{i,j} = v_i - v_j$ is the relative velocity between particles i and j. The expected number of collisions is thus

$$\#\text{collisions} = \sum_{i=1}^{N}\sum_{j=1}^{i-1} w_p P_{i,j} = \sum_{i=1}^{N}\sum_{j=1}^{i-1} w_p \frac{|v_{i,j}|\sigma\Delta t}{V_c}$$

$$\leq \sum_{i=1}^{N}\sum_{j=1}^{i-1} w_p \frac{|v_{i,j}\sigma|_{max}\,\Delta t}{V_c}$$

$$\leq \frac{1}{2} N^2 w_p \frac{|v_{i,j}\sigma|_{max}\,\Delta t}{V_c}$$

The last term is the number of pairs we will select to check for collisions by rejection sampling.

Direct Simulation Monte Carlo (DSMC)

Why is sampling

$$\frac{1}{2} N^2 w_p \frac{|v_{i,j}\sigma|_{max} \Delta t}{V_c}$$

so much better than sampling *N(N-1)/2*? Generally, the factor multiplying N^2 is < 1.

When Δt is "too small" in a cell, the above samples fewer potential collision pairs, sometimes drastically. Δt is a global quantity chosen for the most challenging (collisional) portion of the problem. "Most" of the domain does not need the resolution.

In practice, $|v_{i,j}\sigma|_{max}$ is updated as new $|v_{i,j}\sigma|$ maximums are found through sampling rather than direct computation.

Direct Simulation Monte Carlo (DSMC)

Basic NTC DSMC iteration to advance from time step *n* to *n+1*:

1. Move particles over Δt with their velocities v_i,

$$x_i^{n+1} = x_i^n + \Delta t v_i^n$$

2. In each cell compute the number of potential collision pairs to check,

$$\frac{1}{2} N^2 w_p \frac{|v_{i,j}\sigma|_{max} \Delta t}{V_c}$$

3. Randomly choose pairs and determine if they collide via rejection sampling,

$$|v_{i,j}\sigma| > \text{rand}(0,1)|v_{i,j}\sigma|_{max} \rightarrow \text{collide}$$

   If they collide, update post-collision velocities.

Direct Simulation Monte Carlo (DSMC)

Sandia National Laboratories

Requirements/assumptions for employing NTC DSMC include:

1. Cell size must resolve the collision mean free path λ_{mfp},

$$\Delta x < \lambda_{mfp} = \frac{1}{n\sigma}$$

2. Time step must resolve collision frequency ν_c (this is usually a natural consequence of (1) but is good to check),

$$\Delta t < \nu_c^{-1} = \frac{\lambda_{mfp}}{v} = \frac{1}{n\sigma v}$$

These constraints would ideally apply to the most extreme constraints (minimum λ_{mfp} and maximum ν_c), but because particle properties are stochastic this cannot be guaranteed. This is a recurring theme in kinetic particle methods.

Surface Models

Each surface in the domain typically needs a particle-surface boundary condition for each particle type as well as an electrostatic boundary condition for Poisson's equation. Additionally, surfaces can be given additional particle boundary conditions that generate/emit particles. LOTS of variety.

1D:

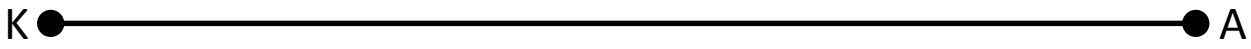

2D and axisymmetric:

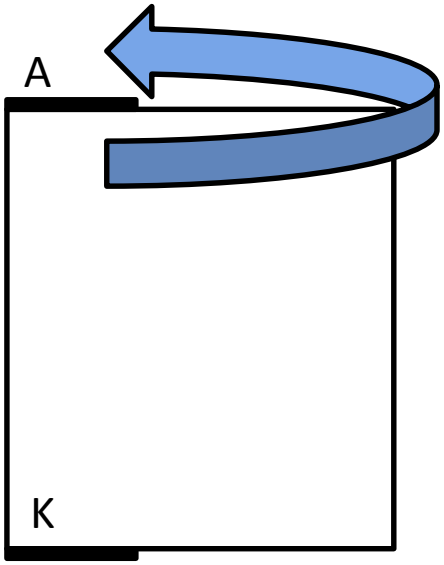

3D:

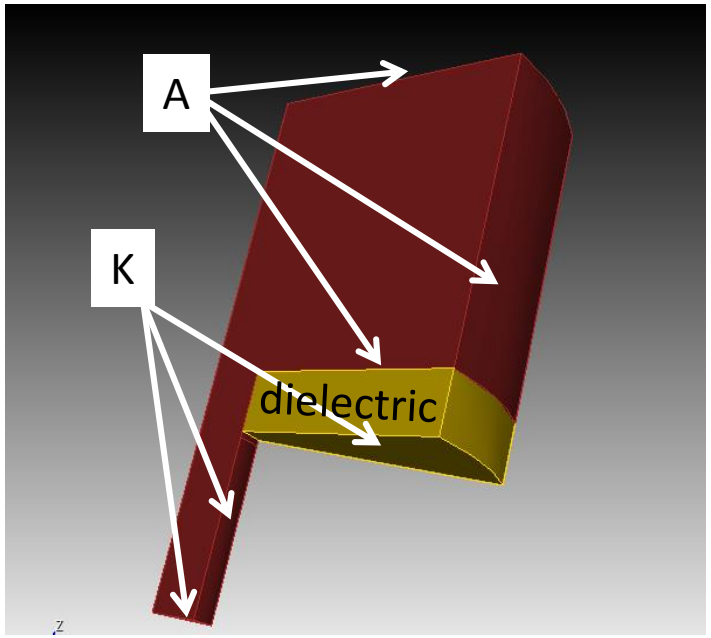

Sandia National Laboratories

BREAK?

Examples

Sandia National Laboratories

We “jump” and move to recent and current vacuum discharge simulations.

Mostly SNL, some HIP/CERN.

LOTS of advanced/specialized techniques.

“Ugly” truth: most “vacuum” arc models have some amount of neutrals laid in or artificially/phenomenologically injected. It is *not well understood* how the first particles are introduced. However, at a non-zero temperature, there must be some particles in the gas region. Real surfaces are “dirty” (e.g., water, residual material).

There is a theme that the model problem (mathematical description) sets up a more challenging problem than reality.

1D Vacuum Arc

Sandia National Laboratories

The following is work based on a collaboration between SNL, Univ. Helsinki, and CERN (cf. Helga Timko's dissertation). One of our goals was to compare code results for the "same" 1D arc problem.

1D Vacuum Arc

Sandia National Laboratories

Injection "cathode"

$f_{Cu} = 10^{22}/cm^2/s$

$f_e = 10^{24}/cm^2/s$

$v_{Cu} = v_e = 0 m/s$

$T_e = 2.9 \times 10^3 K$

$T_{Cu} = 2.9 \times 10^6 K$ (250 eV)

$V = 0V$

Side walls

$dV/dn = 0$

specular

Wall "anode"

$V = 10kV$

Both "electrode" surfaces sputter

e- → Cu (2.9 x 10^6K) at 1% yield

Cu+ → Cu (2.9 x 10^6K) at 100% yield

Cu is also reflected specularly

One bulk reaction

e- + Cu → e- + Cu+ + e-

Simulation parameters

$\Delta x = 0.5$ um

$\Delta t = 1$ fs

Two solutions:

- Fixed particle weight
- Dynamic particle weight (Merge + Clone)

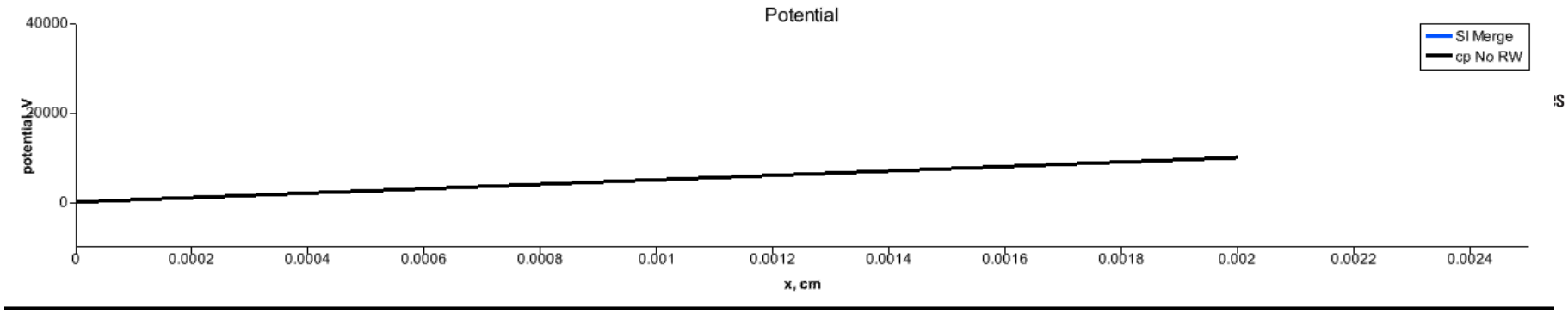
Potential
40000
20000
0
potential, V
Sl Merge
cp No RW
0
0.0002
0.0004
0.0006
0.0008
0.001
0.0012
0.0014
0.0016
0.0018
0.002
0.0022
0.0024
x, cm

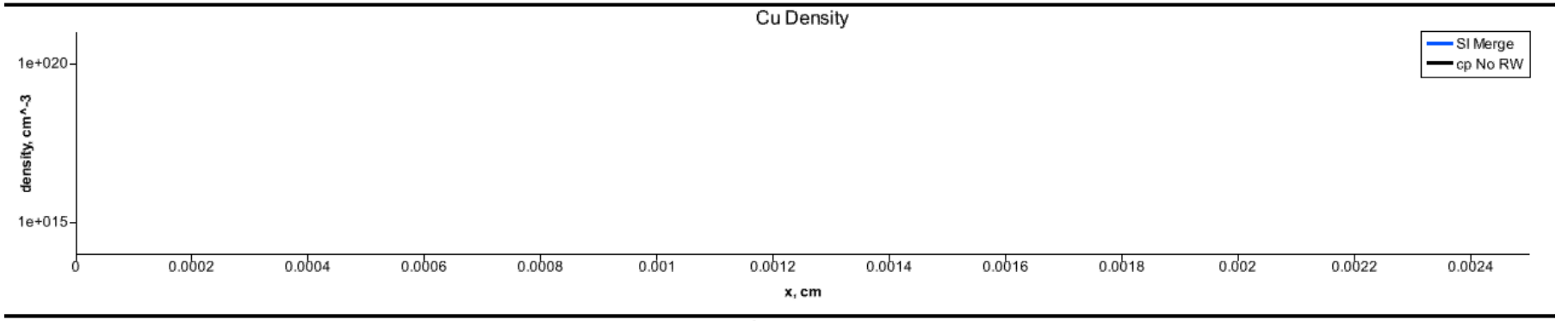
Cu Density
1e+020
1e+015
density, cm^-3
Sl Merge
cp No RW
0
0.0002
0.0004
0.0006
0.0008
0.001
0.0012
0.0014
0.0016
0.0018
0.002
0.0022
0.0024
x, cm

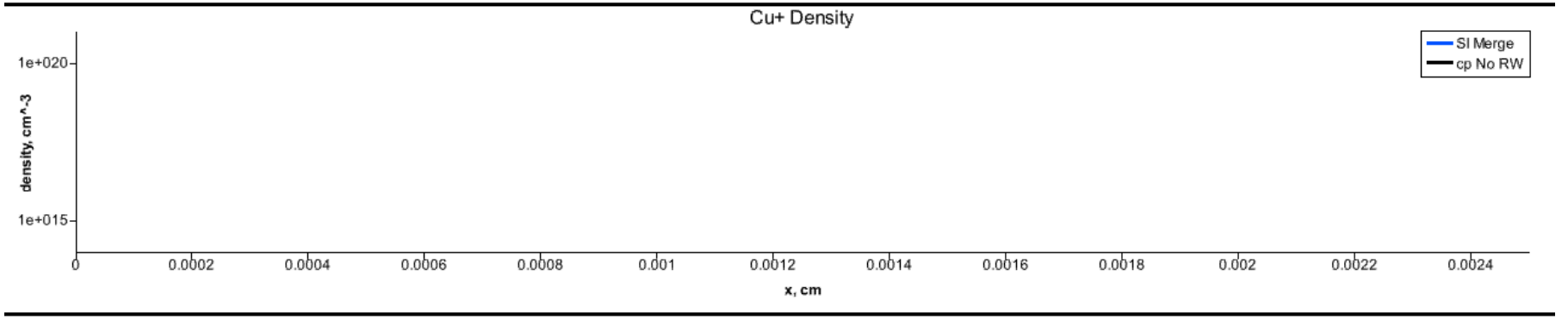
Cu+ Density
1e+020
1e+015
density, cm^-3
Sl Merge
cp No RW
0
0.0002
0.0004
0.0006
0.0008
0.001
0.0012
0.0014
0.0016
0.0018
0.002
0.0022
0.0024
x, cm

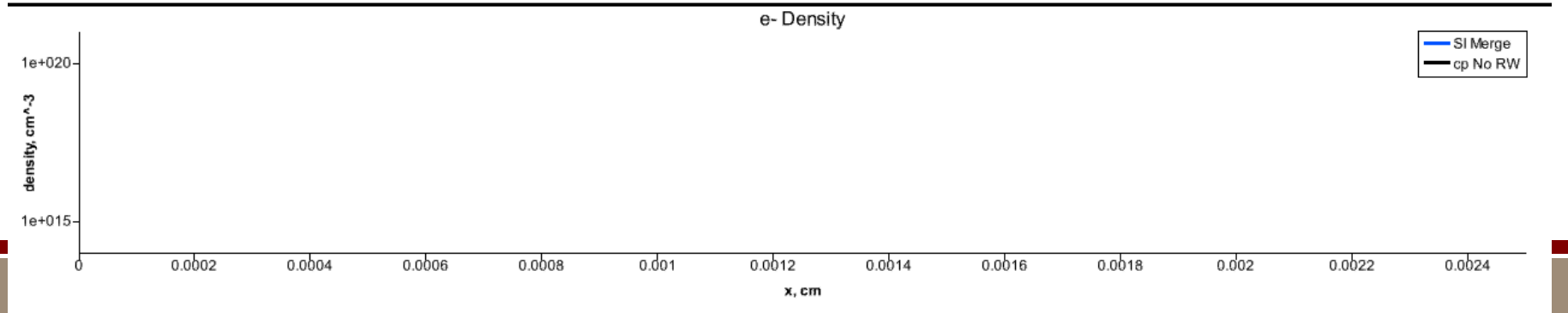
e- Density
1e+020
1e+015
density, cm^-3
Sl Merge
cp No RW
0
0.0002
0.0004
0.0006
0.0008
0.001
0.0012
0.0014
0.0016
0.0018
0.002
0.0022
0.0024
x, cm

1D Vacuum Arc

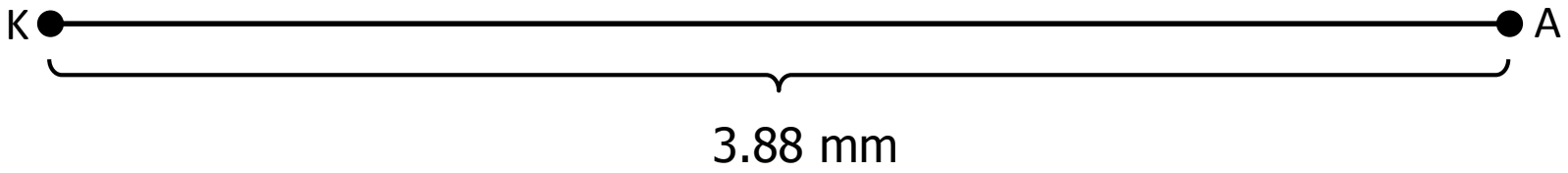

120 V drop across 3.88 mm,
1 Torr background Cu,
Trickle influx of cold e- (10^{10} #/cm^2/μs), 300 K Cu "sputters" at:
1% vs. e-,
100% vs. Cu and Cu+,
1 eV SEE from Cu+ impact,
Δx = 1.38 μm, 2812 cells.

1D Vacuum Arc

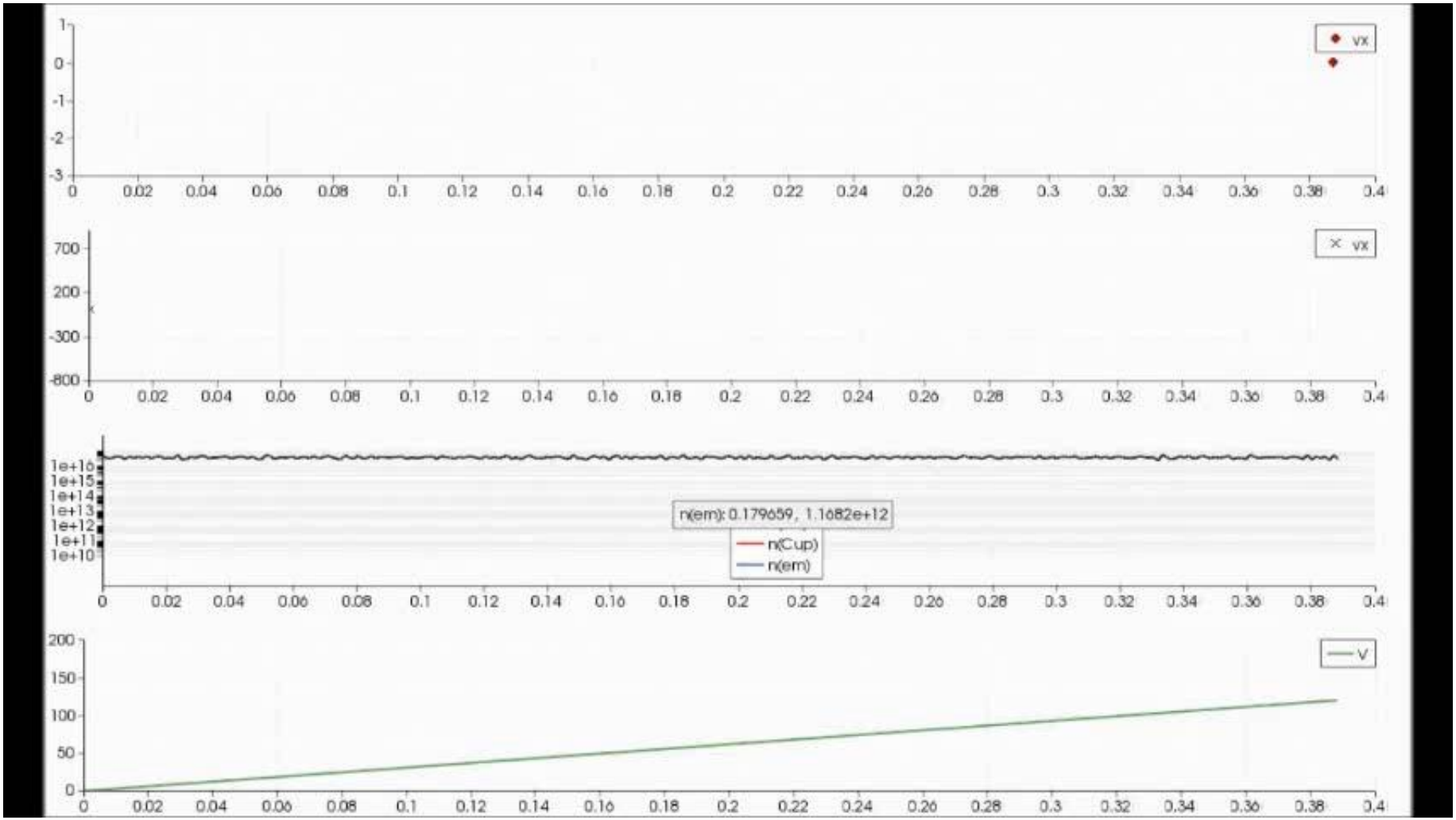

1D Vacuum Arc

t = 166 ns, Δt = 5 ps

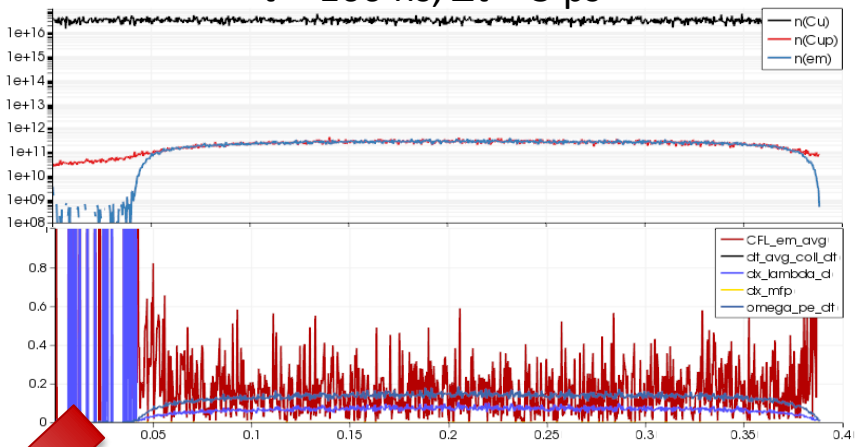

Simulation diagnostics: average e- CFL,
$\Delta t \cdot \nu_c$, $\Delta t \cdot \omega_p$, $\Delta x/\lambda_D$, $\Delta x/\lambda_{mfp}$

t = 236 ns, Δt = 5 ps

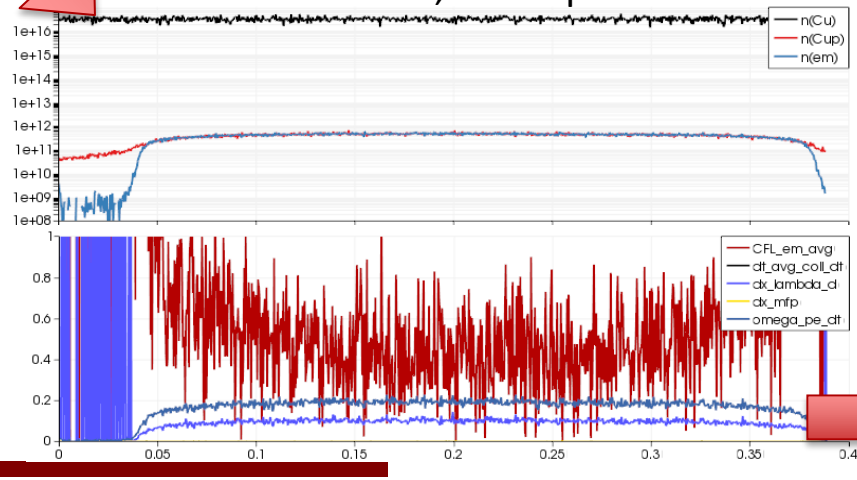

t = 236 ns, Δt = 1 ps

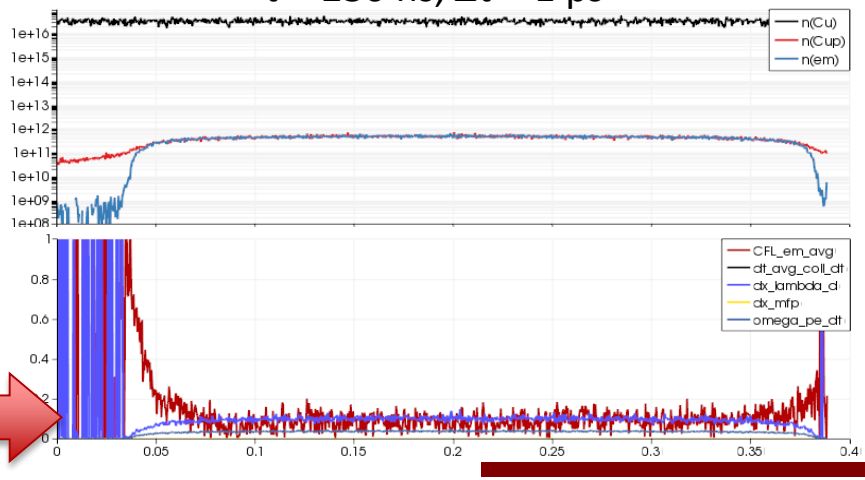

Growing average e- CFL prompts restarting with smaller Δt.

1D Vacuum Arc

Sandia National Laboratories

Injection "cathode"

$f_{Cu} = 10^{22}/cm^2/s$

$f_e = 10^{24}/cm^2/s$

$v_{Cu} = v_e = 0 m/s$

$T_e = 2.9 \times 10^3 K$

$T_{Cu} = 2.9 \times 10^6 K$ (250 eV)

$V = 0V$

?

IMPROVEMENTS

Circuit-driven

Side walls

$dV/dn = 0$

specular

Wall "anode"

$V = 10kV$

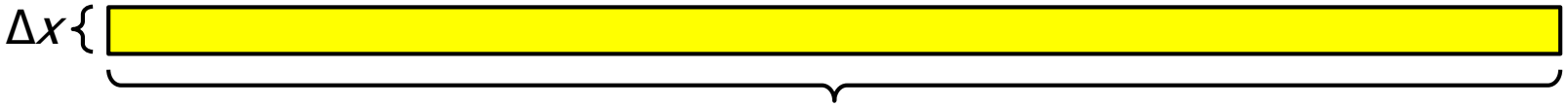

Both "electrode" surfaces sputter

e- → Cu (2.9 x 10^6K) at 1% yield

Cu+ → Cu (2.9 x 10^6K) at 100% yield

Cu is also reflected specularly

One bulk reaction

e- + Cu → e- + Cu+ + e-

Next slides

Simulation parameters

$\Delta x = 0.5$ um

$\Delta t = 1$ fs

Vacuum Arc Electrode Models

Sputtering is energy-dependent.

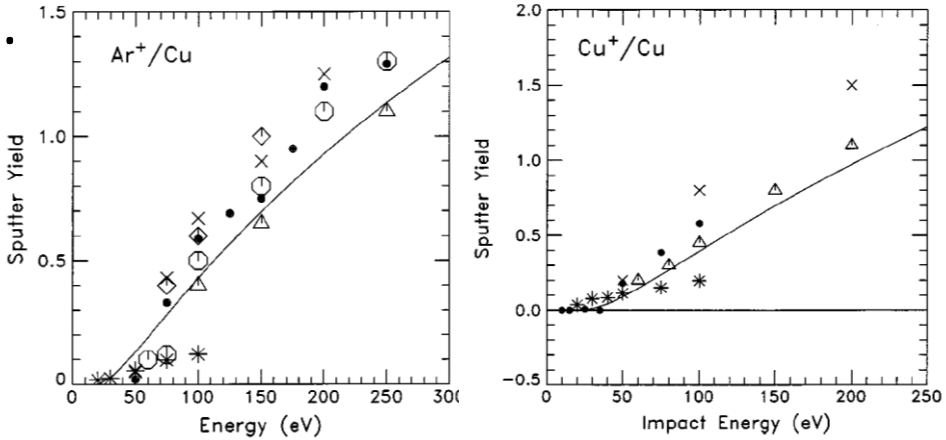

Auger processes?

$$\frac{E_{out}}{E_{in}} = \left[\frac{\cos\alpha \pm (\mu^{-2} - \sin^2\alpha)^{1/2}}{1+\mu^{-1}} \right]^2$$

Secondary electron emission (SEE). Constant yield vs. energy-dependent vs. energy-and-angle-dependent.

$$\gamma(\hat{E}_{inc}, \theta_{inc}) = \gamma_{\max}(\theta_{inc}) \left[\hat{E} e^{(1-\hat{E})} \right]^a,$$

where $\hat{E} = E / E_{\max}$

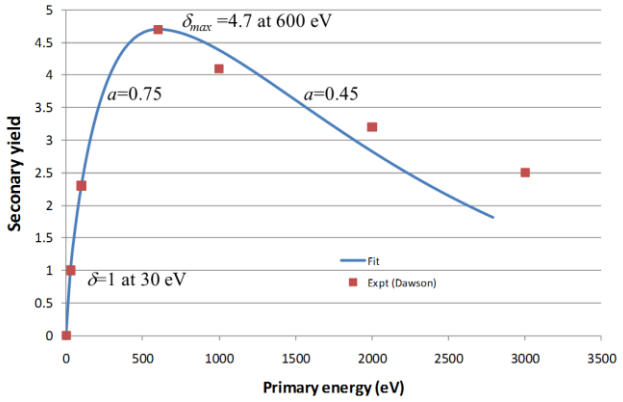

Data interpolation vs. analytic, too!

Vacuum Arc Electrode Models

Electron emission is critical. In reality it is dependent on material (work function), surface field, surface morphology, and surface temperature.

Fowler-Nordheim (FN) accounts for modifying the work function due to large surface electric fields,

$$j_{FN} = \frac{A_{FN}(\beta E_S)^2}{\varphi t^2} e^{-\frac{v_f B_{FN} \varphi^{3/2}}{\beta E_S}} \approx A_{FN}\left(\beta E_S\right)^2 e^{-\frac{B_{FN}}{\beta E_S}}$$

where j_{FN} is the emitted electron current, E_S is the surface field, φ is the material work function, and all other parameters are functions of these or material parameters. In practice, the β value in FN is set much higher than first principles physics would state. FN alone is not a satisfactory model for realistic electron emission.

Vacuum Arc Electrode Models

Schottky thermionic (ST) emission accounts for modifying the work function due to high temperatures,

$$j_{ST} = \lambda_{ST} A_R T_S^2 e^{-\frac{\varphi}{k_B T_S}}$$

The Murphy-Good model incorporates both electric field and thermal modifications to the work function. It is complicated.

None of the above models account for aggregate emission, e.g., exploding tips or other macroparticle emissions. Models in this direction include:

- High-flux sputtering (enhanced emission for high-energy impacting ions/neutrals).
- Ectons (“explosions” at hot locations).

Vacuum Arc Electrode Models

Schottky thermionic (ST) emission accounts for modifying the work function due to high temperatures,

$$j_{ST} = \lambda_{ST} A_R T_S^2 e^{-\frac{\varphi}{k_B T_S}}$$

The Murphy-Good model incorporates both electric field and thermal modifications to the work function. It is complicated.

None of the above models account for aggregate emission, e.g., exploding tips or other macroparticle emissions. Models in this direction include:

- High-flux sputtering (enhanced emission for high-energy impacting ions/neutrals).
- Ectons (“explosions” at hot locations).

Vacuum Arc Electrode Models

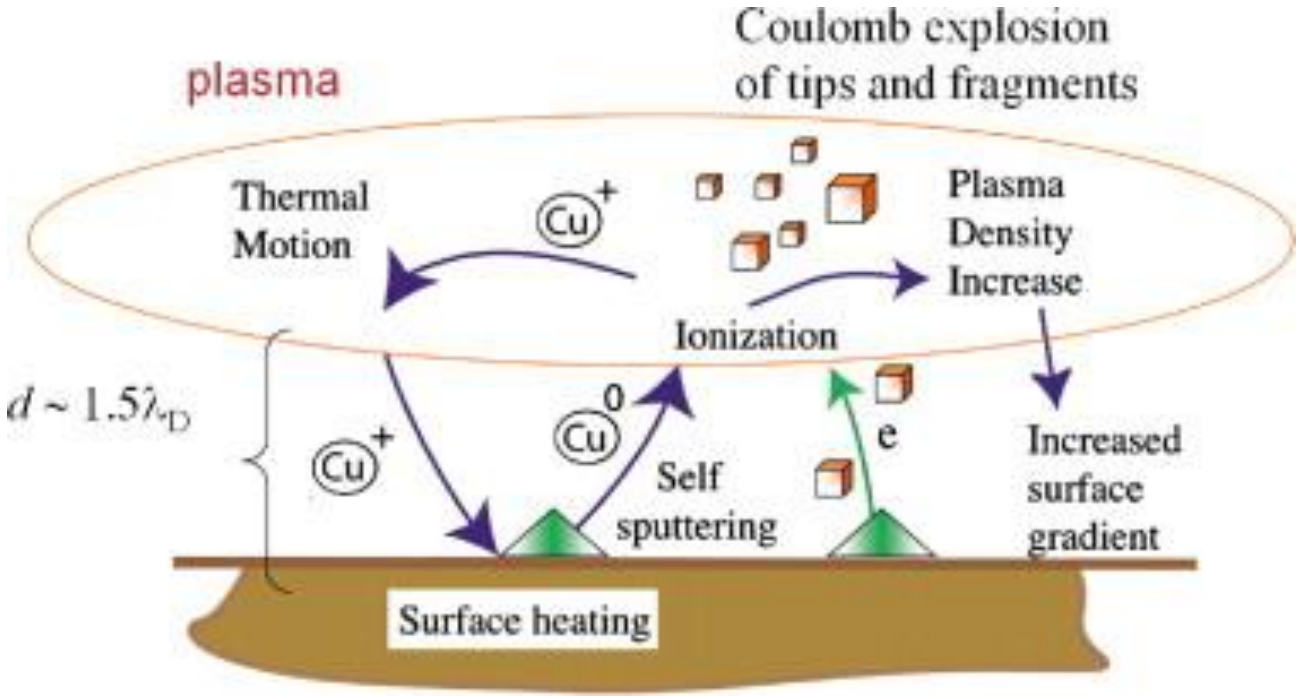

Z. Insepov, J. Norem, S. Veitzer, Atomistic self-sputtering mechanisms of rf breakdown in high-gradient linacs, Nuclear Instruments and Methods in Physics Research Section B: Beam Interactions with Materials and Atoms, Volume 268, Issue 6, 15 March 2010, Pages 642-650.

Plasma Chemistry

$e^- + Cu \rightarrow e^- + Cu^+ + e^-$ is clearly not enough (as expected).

- Electron-neutral elastic scattering reduces available electron energy.
- Excitation reduces available electron energy, too, but makes multi-step ionization possible.
- Charge exchange can lead to fast neutrals.
- Intra-cell Coulomb collisions.
- Multiple charge states? (Seen in experiments.)

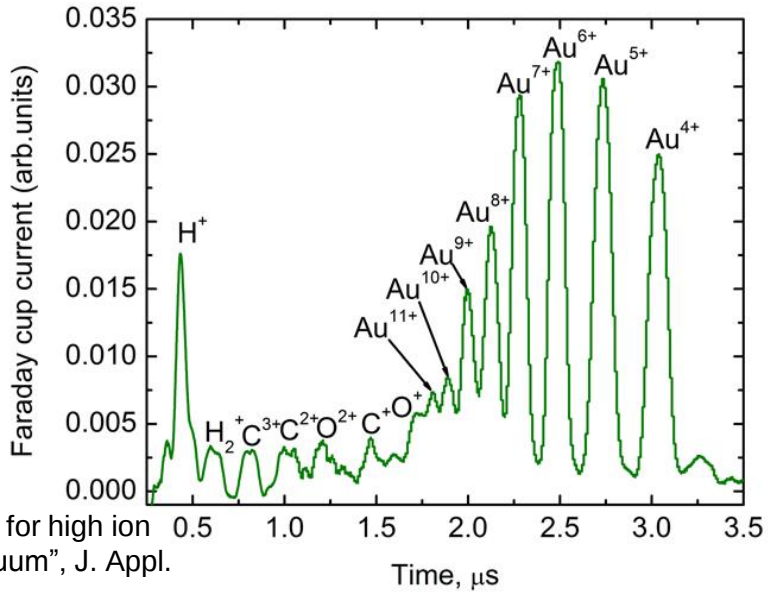

G. Y. Yushkov, A. Anders, "Physical limits for high ion charge states in pulsed discharges in vacuum", J. Appl. Phys., 2009.

2D Vacuum Arc

H. Timko, K. Ness Sjobak, L. Mether, S. Calatroni, F. Djurabekova, K. Matyash, K. Nordlund, R. Schneider, W. Wuensch, “From Field Emission to Vacuum Arc ignition: A New Tool for Simulating Vacuum Arcs”, Contrib. Plasma Phys., 2015.

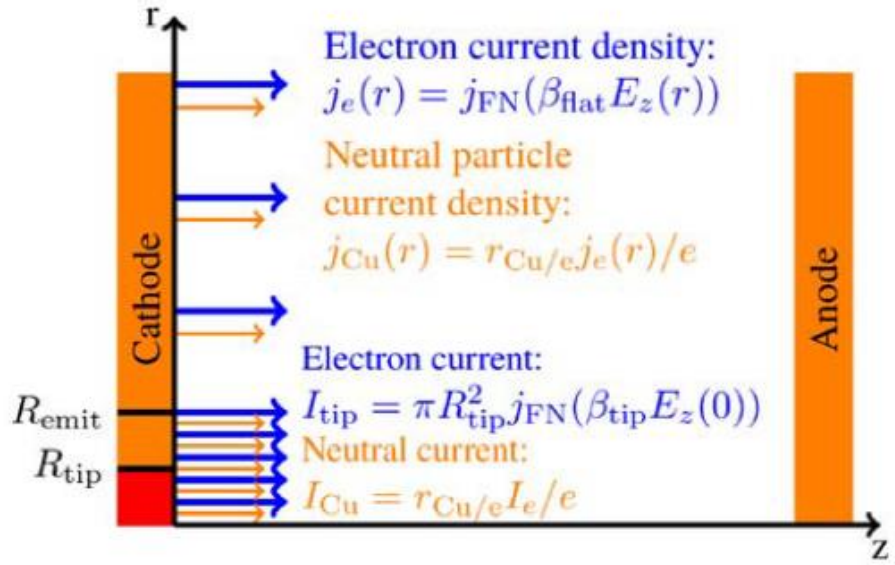

a) Field emission and neutral evaporation.

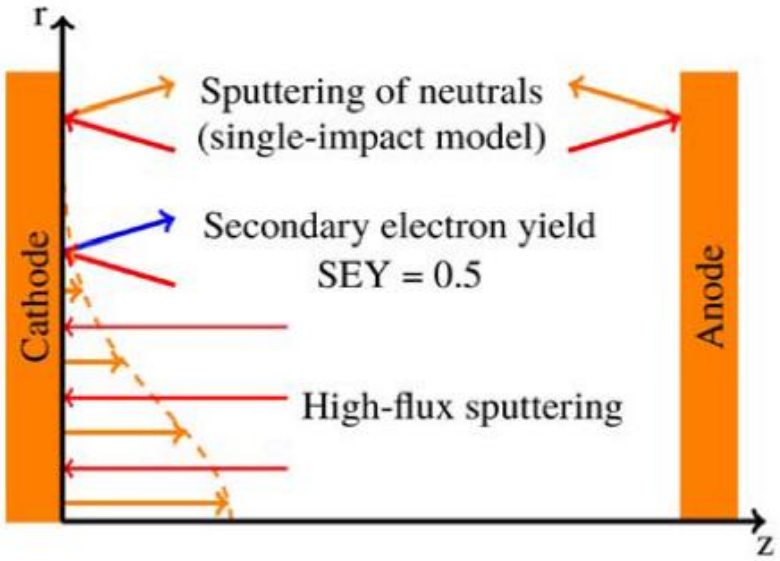

b) Sputtering and secondary electron yield.

2D Vacuum Arc

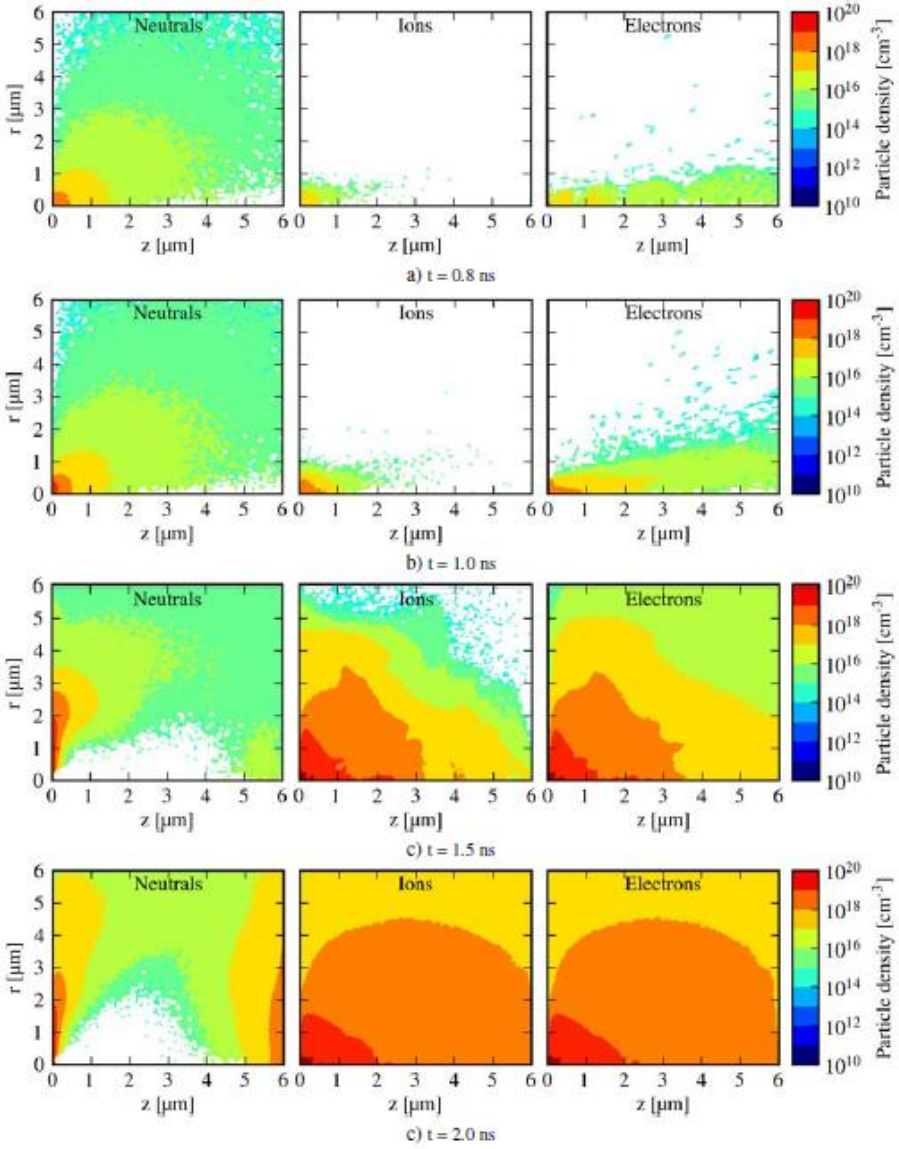

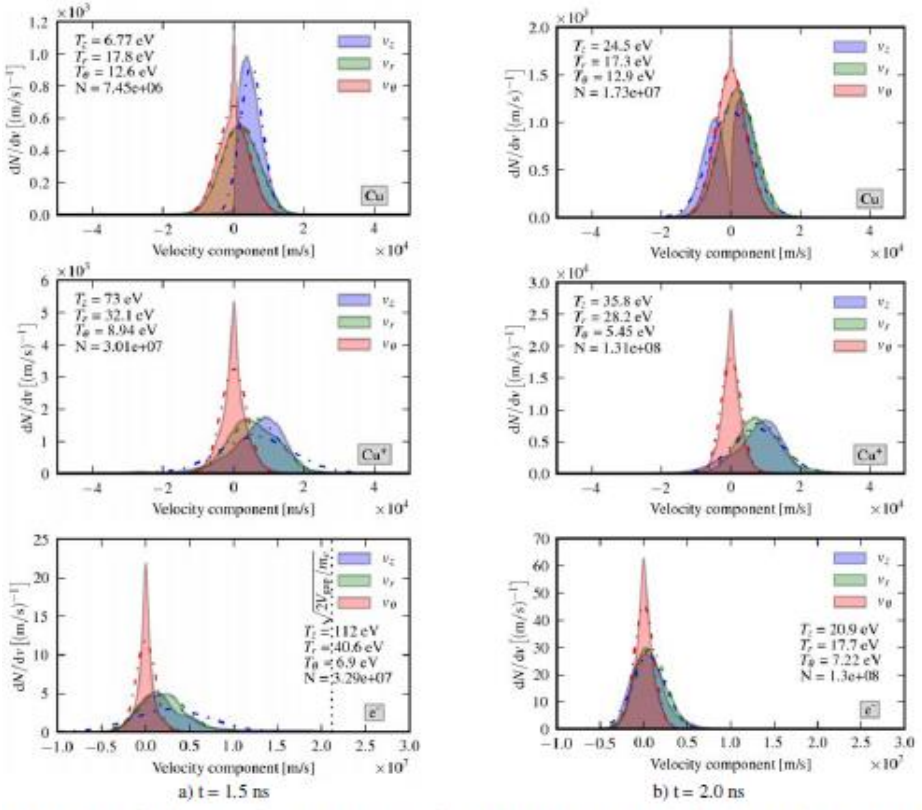

Fig. 8 Velocity distributions and temperatures estimated from the sample variance of the distributions, shown separately for each species and vector component in the reference simulation described in Sec. 4.1. Also plotted is a Gaussian fit with the same mean, variance and normalization as the particle distributions.

H. Timko, K. Ness Sjobak, L. Mether, S. Calatroni, F. Djurabekova, K. Matyash, K. Nordlund, R. Schneider, W. Wuensch, “From Field Emission to Vacuum Arc ignition: A New Tool for Simulating Vacuum Arcs”, Contrib. Plasma Phys., 2015.

3D Vacuum Arc

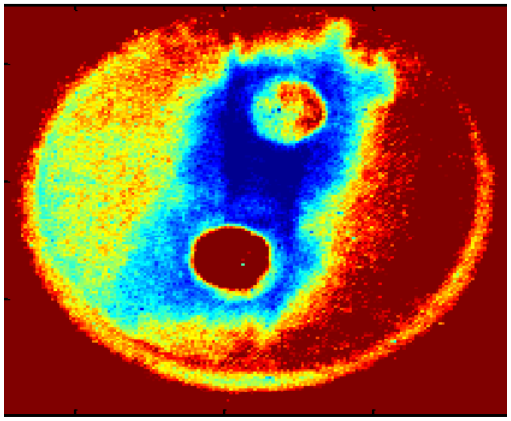

- In vacuum or 4 Torr Ar background
- 1.5 mm inner-to-inner distance
- 0.75 mm diameter electrodes
- Copper electrodes (this picture is Cu-Ti)
- 2 kV drop across electrodes
- 20Ω resistor in series
- Steady conditions around 50V, 100A
- Breakdown time << 100ns
- To meet an ionization mean free path of 1.5 mm at maximum σ, n_i ~ 10^{16} – 10^{17} #/cm^3

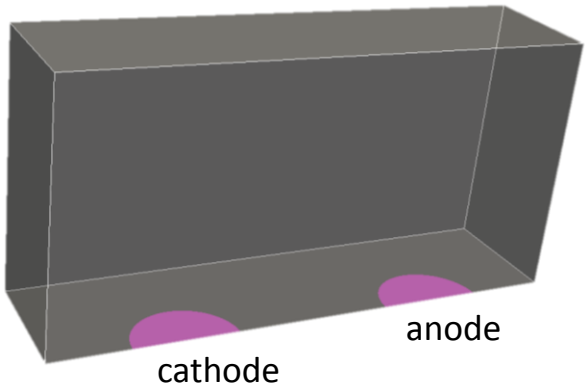

3D computational domain

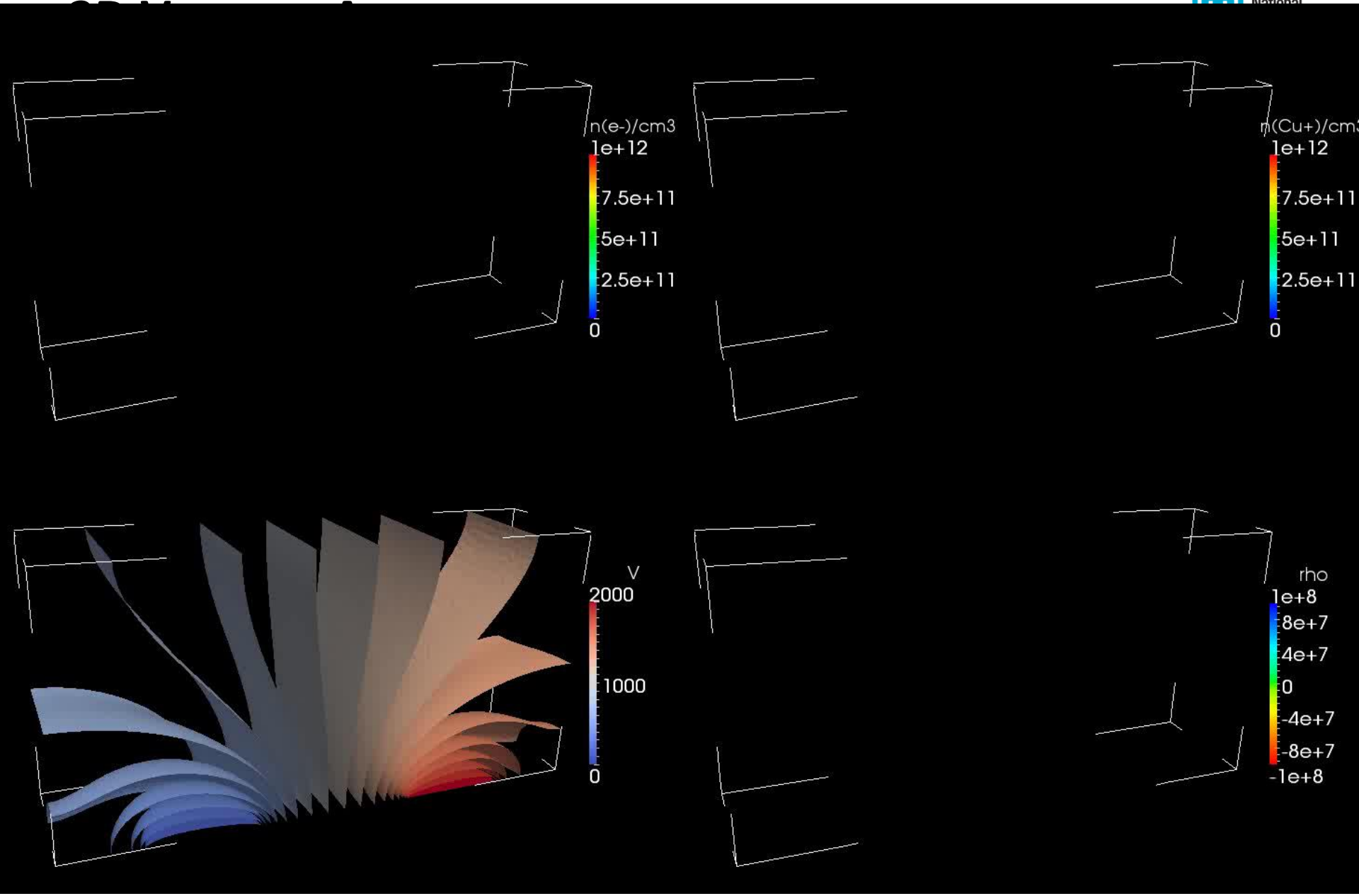
n(e-)/cm3
1e+12
7.5e+11
5e+11
2.5e+11
0
n(Cu+)/cm3
1e+12
7.5e+11
5e+11
2.5e+11
0
V
2000
1000
0
rho
1e+8
8e+7
4e+7
0
-4e+7
-8e+7
-1e+8

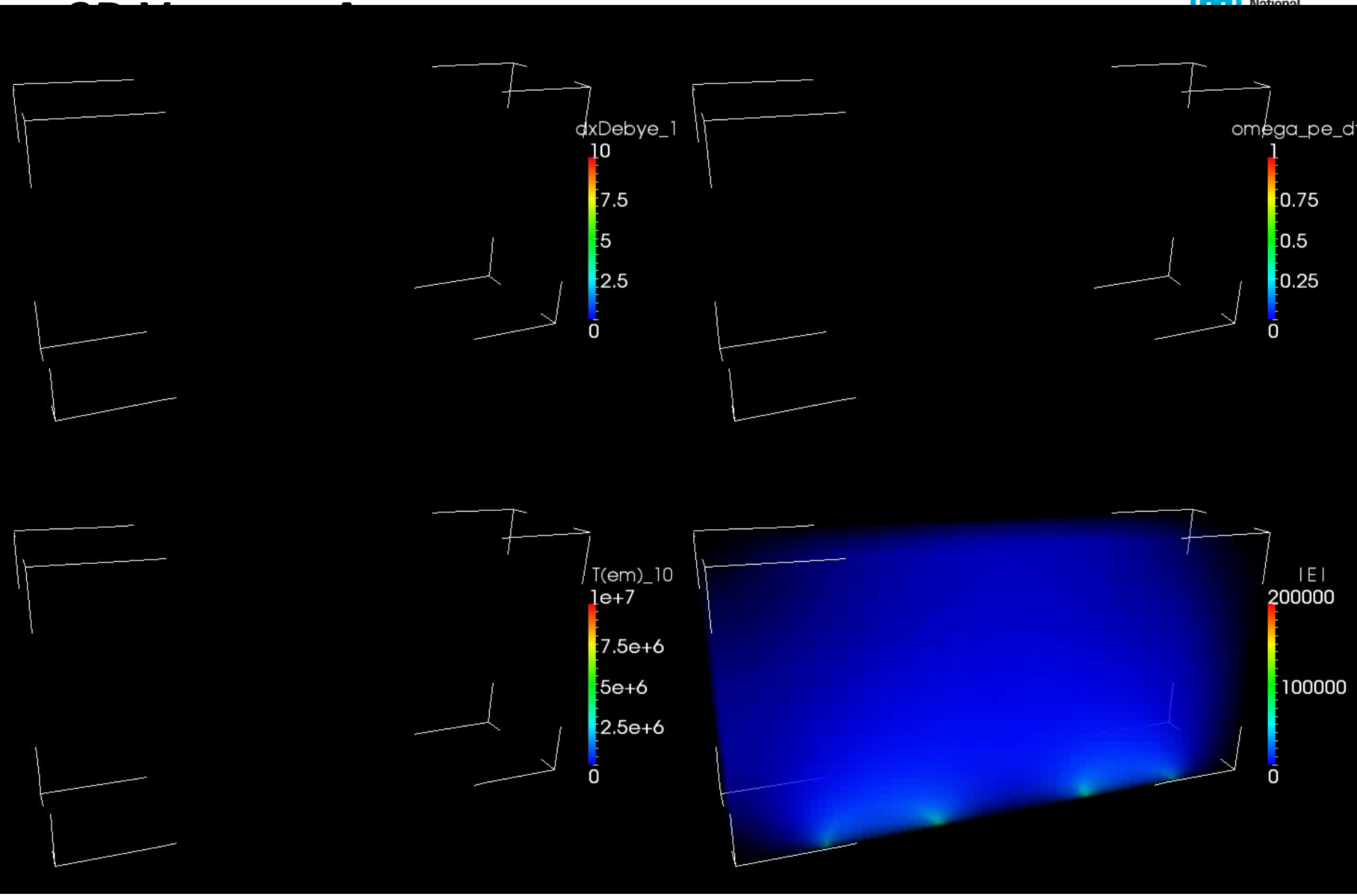
dxDebye_1
10
7.5
5
2.5
0
omega_pe_dt
1
0.75
0.5
0.25
0
T(em)_10
1e+7
7.5e+6
5e+6
2.5e+6
0
| E |
200000
100000
0

Computational Challenges

- Parallel implementations
- Load balancing
- Dynamic particle weighting
- Small particle weights in 3D
- Patch construction (λ_D *vs.* λ_{mfp})
- Complex particle interactions (species, timescales)
- Global adaptive timestep
- Subcycled particle moves
- Explicit vs. semi-implicit vs. implicit
- Circuit model stability
- Output size (Chris Moore current SNL record holder at > 100 TB)
- Visualization
- Post-processing

Recent Advance: Energy Resolution (Chris Moore)

- Examine electron multiplication across gap versus timestep size
  - Space charge ignored when solving for E-field → Plasma frequency not meaningful timestep constraint

- Vary density (collision rate) and hold E/n fixed
  - Neutral collisional simulations exhibit convergence at $\Delta t \sim 1/\nu_c$
  - Error in ionization efficiency results in significant error in steady state plasma density if $\Delta t = 0.5(1/\nu_c)$ is used
  - Charged particle electron avalanche exhibits convergence at $\Delta t \sim 0.01(1/\nu_c)$.

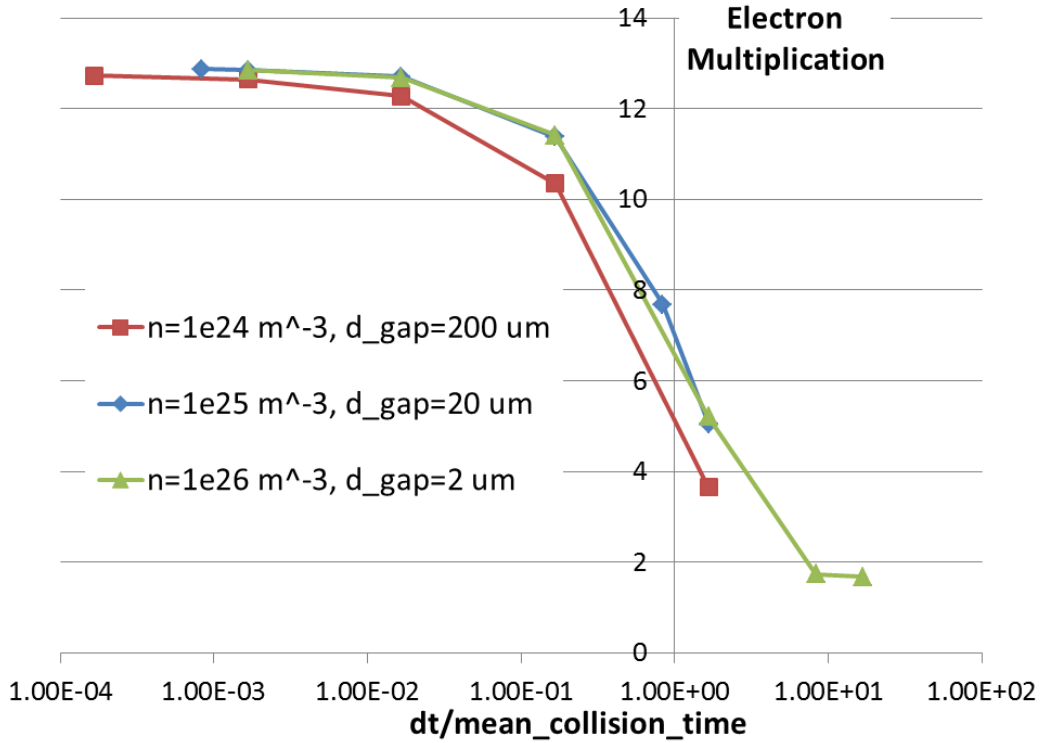

Recent Advance: Energy Resolution (Chris Moore)

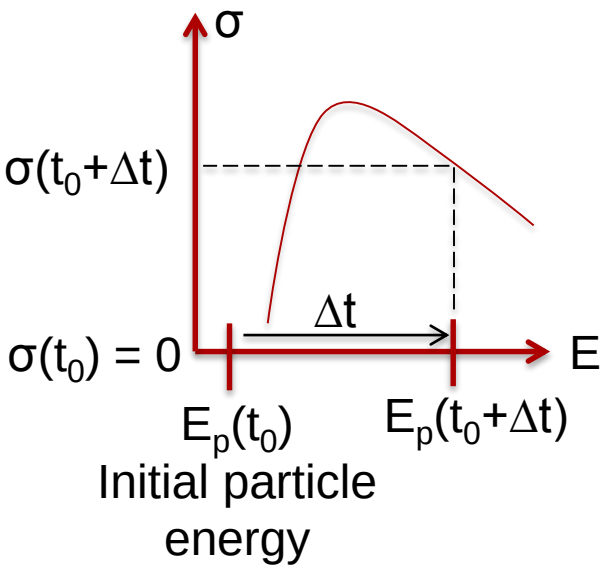

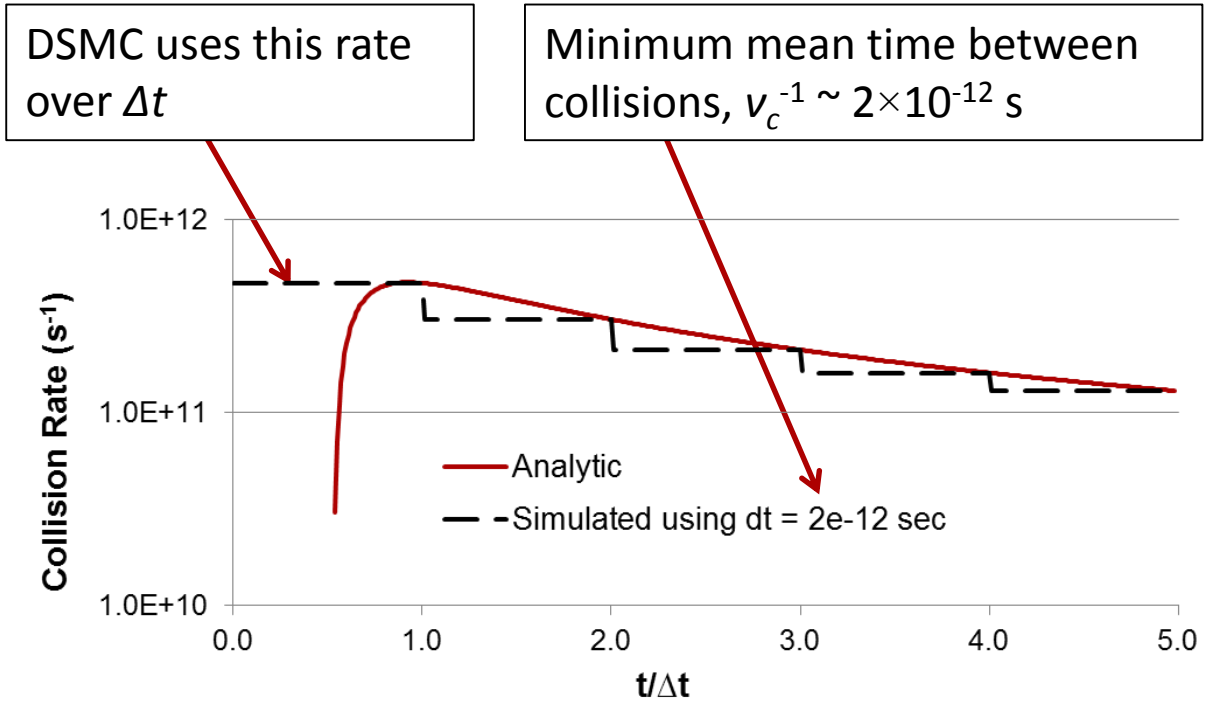

- Large steps in energy caused by large time steps can be seen to result in large error in the simulated collision rate.

Recent Advance: Energy Resolution (Chris Moore)

- Normalized error in the number of collisions for a given Δt and initial particle energy:

$$\overline{\epsilon_{col}}(\Delta t, E_{p,0}) = \frac{1}{\Delta t}\left[\int_{t_0}^{t_f=t_0+\Delta t} n\sigma_{iz}(t)v_p(t)dt - n\sigma_{iz}(t_f)v_p(t_f)\Delta t\right]$$

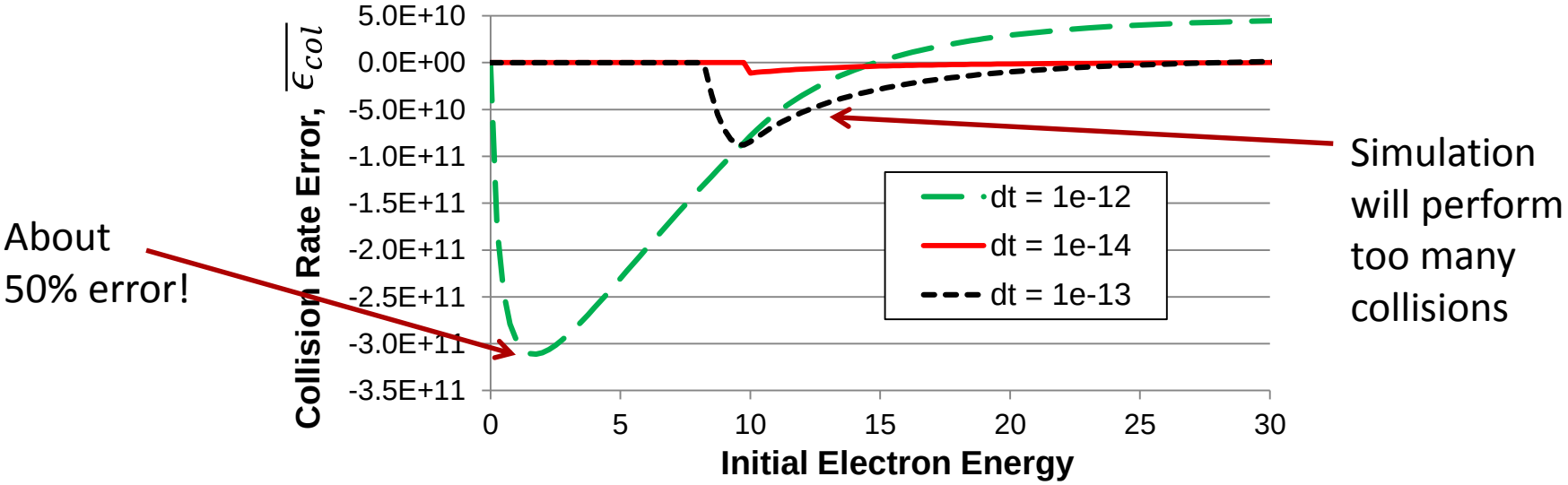

- Error introduced in steady state arc behavior a function of the electron temperature (EEDF) .
  - T_e ~ 1-10 eV for typical discharge so most probable $E_{p,0}$ ~ 10 eV.

References

1. D. C. Montgomery, Theory of the Unmagnetized Plasma. Gordon and Breach, 1971.
2. D. R. Nicholson, Introduction to Plasma Theory (Plasma Physics). Wiley, 1983.
3. R. W. Hockney, J. W. Eastwood, Computer Simulation Using Particles. CRC Press, 1989.
4. C. K. Birdsall, A. B. Langdon, Plasma Physics via Computer Simulation. Taylor & Francis, 2005.
5. G. A. Bird, Molecular Gas Dynamics and the Direct Simulation of Gas Flows. Oxford, 1994.
6. LXcat database of electron cross-sections: www.lxcat.net.
7. H. Timko, P. Crozier, M. Hopkins, K. Matyash, R. Schneider, "Why Perform Code-to-Code Comparisons: A Vacuum Arc Discharge Simulation Case Study", Contrib. Plasma Phys., 2012.
8. P. H. Dawson, "Secondary Electron Emission Yields of some Ceramics", J. Appl. Phys., 1966.
9. R. Forbes, "Physics of generalized Fowler-Nordheim-type equations", J. Vac. Sci. Technol. B, 2008.
10. M. Dionne, S. Coulombe, J.-L. Meunier, "Field emission calculations revisited with Murphy and Good theory: a new interpretation of the Fowler-Nordheim plot", J. Phys. D, 2008.
11. E. L. Murphy, R. H. Good, Jr., "Thermionic Emission, Field Emission, and the Transition Region", Phys. Rev., 1956.
12. H. Timko, K. Ness Sjobak, L. Mether, S. Calatroni, F. Djurabekova, K. Matyash, K. Nordlund, R. Schneider, W. Wuensch, "From Field Emission to Vacuum Arc ignition: A New Tool for Simulating Vacuum Arcs", Contrib. Plasma Phys., 2015.

Sandia National Laboratories

Thank You!

CV & SV & V & SA & UQ

All Interesting Arc/Plasma Behavior Is Nonlinear And Coupled – How Can We Be Confident In Our Predictions?

CV: Code Verification. Necessary, woefully insufficient. Can test single simple capabilities.

SV: Solution … the right solution …

V: Validati… …ality. Ideally, … …tion verificat…

SA: Sensitiv… …ermine which numerical/physical parameters impact the prediction, experimental result, and/or validation comparison. Identifies problem areas and is a source of planning decisions/efficiency.

UQ: Uncertainty Quantification. Estimate uncertainty in a code prediction, usually without experimental comparator. Incorporates error estimation and quantified code prediction uncertainties.

ALL OF THIS IS MORE COMPLICATED BECAUSE OUR BASIC MODELING METHODS ARE STOCHASTIC (PIC, MCC, MD, ...) AND DO NOT HAVE TYPICAL "GRID CONVERGENCE" BEHAVIOR

Our PIC-DSMC Algorithm

Basic algorithm for one time step of length Δt:

1. Given known electrostatic field $\mathbf{E}^n$, move each particle for $\frac{\Delta t}{2}$ via:

$$v_i^{n+1/2} - v_i^n + \frac{\Delta t}{2}\left(\frac{q_i}{m_i}\mathbf{E}^n\right)$$

$$x_i^{n+1} = x_i^n + \Delta t v_i^{n+1/2}$$

2. Compute intersections (non-trivial in parallel).
3. Transfer charges from particle mesh to static mesh.
4. Solve for $\mathbf{E}^{n+1}$

$$\nabla \cdot \left(\epsilon \nabla V^{n+1}\right) - -\rho(\mathbf{x}^{n-1})$$

$$\mathbf{E}^{n+1} = -\nabla V^{n+1}$$

5. Transfer fields from static mesh to dynamic mesh.
6. Update each particle for another $\frac{\Delta t}{2}$ via:

$$v_i^{n+1} - v_i^{n+1/2} + \frac{\Delta t}{2}\left(\frac{q_i}{m_i}\mathbf{E}^{n-1}\right)$$

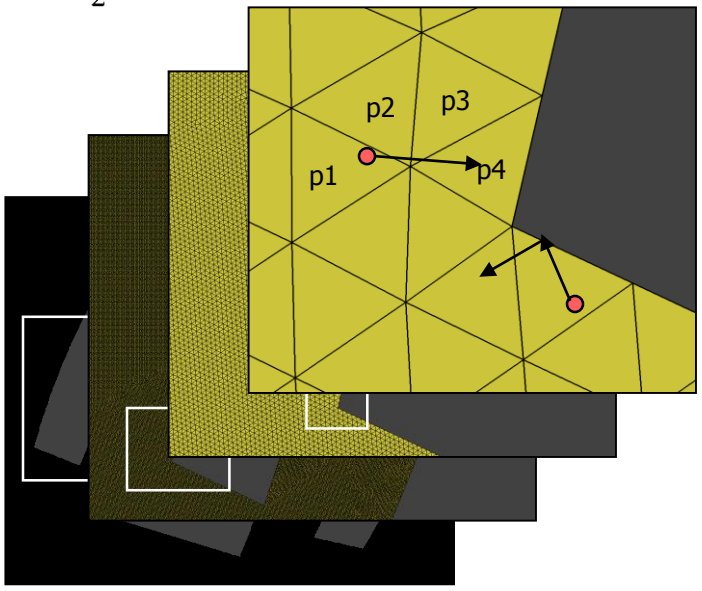

7. Perform DSMC collisions: sample pairs in element, determine cross section and probability of collision. Roll a digital die, and if they collide, re-distribute energy.
8. Perform chemistry: for each reaction, determine expected number of reactions. Sample particles of those types, perform reaction (particle creation/deletion).
9. Reweight particles.
10. Compute post-processing and other quantities and write output.
11. Rebalance particle mesh if appropriate (variety of determination methods).

Surface Models (Electrostatic)

Dirichlet: $V = \langle value \rangle$, $V = 0$ is popular.

Neumann: $dV/dn = E \cdot n = \langle value \rangle$, $E \cdot n = 0$ is popular.

Circuit: $V(t) = V_{PS} + I(t)R$

$$V(t) = V_{PS} + I(t)R + L\frac{dI(t)}{dt} + \frac{1}{C}\int^{t} I(\tau)d\tau$$

where $I(t)$ is the particle-based current through some surface, V_{PS} is some applied voltage (e.g., from power supply), R, L, and C, are resistance, conductance, and capacitance, respectively.

Surface charging will occur at dielectric surfaces and require treatment in the Poisson solver for

$$\sigma_S(t) = q_S(t)/A_S$$

where $q_S(t)$ is accumulated particle charge and A_S is the area.

The Truth about Particle Weights

In 3D particle weights can become < 1…

T_e = 5 eV, n_e = 10^{17}/cm^3 →
λ_D ~ 5 x 10^{-6} cm →
dx ~ (5/3) x 10^{-6} cm →
tetrahedron volume ~ 6 x 10^{-19}/cm^3.

A single computational particle of weight 1 represents a number density of 6 x 10^{-19}/cm^3 (compare to n_e). In 2D with a 1 cm "depth", the triangle-based volume ~ 1 x 10^{-12}/cm^3, which is just fine.

Is this a strongly coupled plasma? The plasma parameter = Λ= # particles in a Debye sphere ~ 60. However at n_e = 10^{19}/cm^3, T_e = 2 eV, Λ= 1.5. $\Lambda << 1$ and $\Lambda >> 1$ are the clear cases.